Cancer Biology

# DHODH inhibition enhances the efficacy of immune checkpoint blockade by increasing cancer cell antigen presentation

**Nicholas J. Mullen, Surendra K. Shukla, Ravi Thakur, Sai Sundeep Kollala, Dezhen Wang, Nina Chaika, Juan F. Santana, William R. Miklavcic, Drew A. LaBreck, Jayapal Reddy Mallareddy, David H. Price, Amarnath Natarajan, Kamiya Mehla, David B. Sykes, Michael A. Hollingsworth, Pankaj K. Singh**

Eppley Institute for Research in Cancer and Allied Diseases, University of Nebraska Medical Center, Omaha, NE 68198-5950, USA • Department of Oncology Science, University of Oklahoma Health Sciences Center, Oklahoma City, OK, 73014, USA • Department of Biochemistry and Molecular Biology, University of Iowa, Iowa City, Iowa, USA • Center for Regenerative Medicine, Massachusetts General Hospital, Boston, MA, USA • Harvard Stem Cell Institute, Cambridge, MA, USA • Department of Pathology, University of Oklahoma Health Sciences Center, Oklahoma City, OK, 73104, USA • OU Health Stephenson Cancer Center, University of Oklahoma Health Sciences Center, Oklahoma City, OK, 73104, USA



**Reviewed Preprint**

Revised by authors after peer review.

About eLife's process

**Reviewed preprint version 2**
April 5, 2024 (this version)

**Reviewed preprint version 1**
May 23, 2023

**Posted to preprint server**
April 5, 2023

**Sent for peer review**
April 3, 2023

## Abstract

Pyrimidine nucleotide biosynthesis is a druggable metabolic dependency of cancer cells, and chemotherapy agents targeting pyrimidine metabolism are the backbone of treatment for many cancers. Dihydroorotate dehydrogenase (DHODH) is an essential enzyme in the de novo pyrimidine biosynthesis pathway that can be targeted by clinically approved inhibitors. However, despite robust preclinical anticancer efficacy, DHODH inhibitors have shown limited single-agent activity in phase 1 and 2 clinical trials. Therefore, novel combination therapy strategies are necessary to realize the potential of these drugs. To search for therapeutic vulnerabilities induced by DHODH inhibition, we examined gene expression changes in cancer cells treated with the potent and selective DHODH inhibitor brequinar (BQ). This revealed that BQ treatment causes upregulation of antigen presentation pathway genes and cell surface MHC class I expression. Mechanistic studies showed that this effect is 1) strictly dependent on pyrimidine nucleotide depletion, 2) independent of canonical antigen presentation pathway transcriptional regulators, and 3) mediated by RNA polymerase II elongation control by positive transcription elongation factor B (P-TEFb). Furthermore, BQ showed impressive single-agent efficacy in the immunocompetent B16F10 melanoma model, and combination treatment with BQ and dual immune checkpoint blockade (anti-CTLA-4 plus anti-PD-1) significantly prolonged mouse survival compared to either therapy alone. Our results have important implications for the clinical development of DHODH inhibitors and provide a rationale for combination therapy with BQ and immune checkpoint blockade.

**eLife assessment**

This **important** study reports a novel mechanism linking DHODH inhibition and subsequent pyrimidine nucleotide depletion with upregulation of cell surface MHC I in cancer cells. The in vitro mechanistic data isarecompelling, with rigorous methodology and validation across multiple cell lines. The authors also provide in vivo evidence for additive effects of DHODH inhibitors and immune checkpoint blockade. However, the in vivo assessments of the functional relevance of this mechanism remain **incomplete**, requiring additional analyses to fully substantiate the conclusions made.

# Introduction

Deranged cellular metabolism is a universal feature of cancer cells [1,2]. One particularly cancer-essential metabolic aberration is the hyperactive synthesis and utilization of nucleotide triphosphates; this phenotype is a critical driver of cancer cell malignant behaviors, including uncontrolled proliferation, evasion of the host immune response, metastasis to distant organs, and resistance to antineoplastic therapy [3]. The de novo pyrimidine biosynthesis pathway, which generates pyrimidine nucleotides from aspartate and glutamine, is consistently hyperactive in cancer cells and druggable by clinically approved inhibitors [4]. Dihydroorotate dehydrogenase (DHODH) catalyzes the fourth step in this pathway and is essential for de novo pyrimidine synthesis. DHODH inhibitors have shown robust preclinical anticancer activity across diverse cancer types [5-14] and have recently entered clinical trials for multiple hematologic cancers (NCT04609826 and NCT02509052). Although there is a vast literature on DHODH inhibitors dating back to the early 1990s, and despite the "rediscovery" of DHODH in recent years as a critical cancer cell metabolic dependency, important questions about the cellular response to DHODH inhibition remain unanswered.

While combination chemotherapy is highly effective and potentially curative against certain cancers (e.g. Hodgkin lymphoma, testicular cancer, childhood leukemia, and others), many common malignancies are refractory to chemotherapy (e.g. lung cancer, pancreatic cancer, colorectal cancer, etc.) [15]. In some chemotherapy-refractory cancers (most prominently melanoma, mismatch repair deficient colorectal cancer, bladder cancer, and non-small cell lung cancer), immunotherapeutic strategies have demonstrated strong efficacy and led to durable remissions in a subset of patients [16]. The efficacy of immunotherapy agents is dependent on multiple factors, including tumor antigen presentation, limited immune cells in the tumor milieu, and T-cell activation status [17,18]. Adoptive cell therapies and immune checkpoint blockade (ICB) can address the issues of limited immune cell recruitment into tumors and limited T-cell activation, respectively. However, adequate antigen presentation by tumor cells is still required for immunotherapy efficacy, which relies on T-cell-mediated adaptive immunity.

The antigen presentation pathway (APP) mediates the presentation of endogenous peptide antigens to CD8 T-cells via MHC class I (MHC-I). This pathway entails the degradation of cellular proteins into small peptides by the proteasome, the import of these peptides into the endoplasmic reticulum by transporter associated with antigen presentation proteins (*TAP1* and *TAP2*), and the loading of these peptides into the MHC-I complex, which consists of a heavy chain (encoded by *HLA-A*, *HLA-B*, or *HLA-C*) and a light chain (encoded by *B2M*) [19]. APP genes are often downregulated in cancer cells, and this impedes the recognition of immunogenic MHC-I restricted cancer cell antigens by infiltrating T-cells [20]. Antigen presentation and T-cell recognition are crucial for T-cell-mediated killing of cancer cells [21-23], and forced MHC-I expression enhances

immunotherapy efficacy in preclinical models [24-27]. Furthermore, high tumoral expression of MHC-I, MHC-II, and other APP genes correlates with better overall survival in patients with melanoma treated with ICB therapies [28-31].

While previous reports have shown that pyrimidine nucleotide depletion triggers the expression of innate immunity-related genes and induces an interferon-like response [32-34], the role of pyrimidine starvation in antigen presentation has not been reported. Herein, we report that DHODH inhibition induces the robust upregulation of APP genes and increases tumor cell antigen presentation via MHC-I. We further explored the mechanism and functional consequences of DHODH inhibitor-mediated APP induction in cancer.

# Results

## Brequinar induces upregulation of MHC-I and antigen presentation pathway genes

We examined gene expression changes following transient or prolonged DHODH inhibition by culturing human pancreatic ductal adenocarcinoma cell lines S2-013 and CFPAC-1 in the presence of BQ at two different doses for 16 hours and for a two-week duration (**Fig 1A**). Gene set enrichment analysis (GSEA) using Hallmark and KEGG gene sets from MSigDB [35,36] revealed 17 gene sets that were significantly upregulated (FDR q < 0.25) across both cell lines following two-week BQ exposure (**Fig 1B**). Twelve of these gene sets (highlighted in purple) are ontologically related to antigen presentation and contain MHC class I, MHC class II, and/or APP genes such as *TAP1* in the leading edge. Certain gene sets, such as allograft rejection (KEGG), graft versus host disease (KEGG), and antigen processing and presentation (KEGG) are composed almost entirely of APP genes (**Fig 1C**). Heatmap analysis showed that APP genes were robustly upregulated in a dose- and duration-dependent manner in CFPAC-1 (**Fig 1D**) and S2-013 (Fig S1A) cells. The effect size was generally smaller for S2-013 cells, likely because they are resistant to DHODH inhibition due to efficient nucleoside salvage, as we previously reported [37]. Publicly available RNA-seq data from human A375 melanoma cells treated with the clinically approved DHODH inhibitor teriflunomide [38] corroborated our findings, as teriflunomide caused a rapid (within 12 hours) and duration-dependent increase in MHC-I/II and APP transcript levels (**Fig 1E**).

We validated these gene expression changes in CFPAC-1 cells by RT-qPCR (Fig S1B) and then performed RT-qPCR to assess the mRNA levels of genes coding for MHC-I across a panel of human cancer cell lines treated with BQ for 24 hours (**Fig 1F**). This confirmed that MHC-I heavy chain transcripts (*HLA-A*, *HLA-B*, and *HLA-C*) are consistently upregulated in response to BQ across diverse cancer types (**Fig 1F**). To optimize conditions for *in vivo* studies, we tested the long-term response and observed that two-week BQ treatment of B16F10 murine melanoma cells also caused dramatic APP gene upregulation (Fig S1C). Flow cytometry confirmed a marked increase in cell surface MHC-I levels in nonpermeabilized live CFPAC-1 (**Fig 1G**) and B16F10 (**Fig 1H**) cells following a two-week BQ treatment, confirming that transcriptional upregulation of APP genes results in greater cell surface antigen presentation.

In parallel, we confirmed pyrimidine nucleotide depletion upon treatment with BQ at different doses by performing metabolomics analysis of CFPAC-1 and B16F10 cells following BQ treatment. The results demonstrated a rapid (8-hour treatment) and dose-dependent accumulation of dihydroorotate and N-carbamoyl-aspartate (upstream of DHODH) as well as depletion of pyrimidine nucleotides UTP and CTP (**Fig 1I-J**) and other pyrimidine species (Fig S1D-E). These results confirm that on-target DHODH inhibition and resultant pyrimidine nucleotide depletion correlates with the transcriptional induction of APP genes and enhanced antigen presentation via MHC-I.

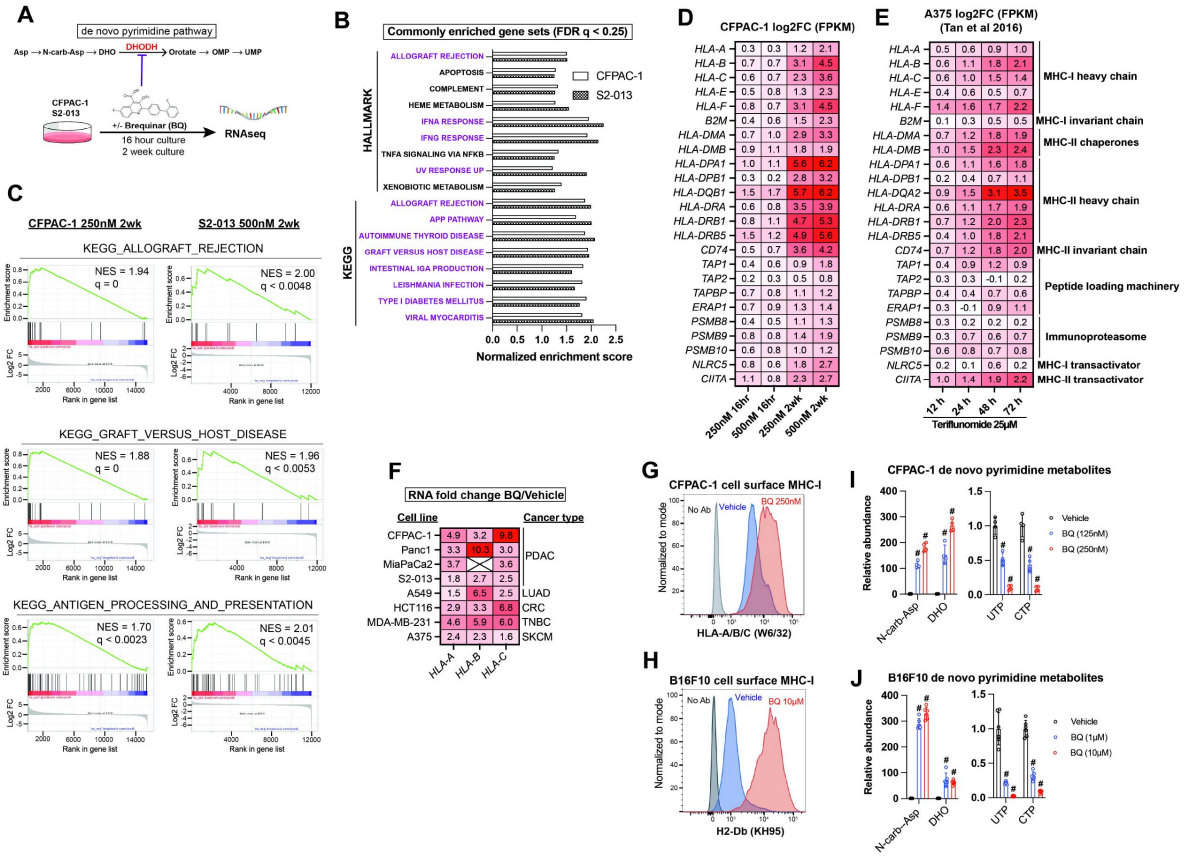


## Figure 1

### Brequinar induces mRNA expression of antigen presentation pathway genes and upregulates cell surface MHC-I in diverse cancer cell lines.

**A)** Schematic of RNA sequencing experiment for panels C-D, with de novo pyrimidine pathway shown to highlight the role of DHODH **B)** Normalized enrichment scores for gene sets commonly enriched (FDR q < 0.25) in S2-013 (500nM) and CFPAC-1 (250nM) cells following two-week BQ treatment, as assessed by gene set enrichment analysis. **C)** GSEA plots for indicated gene sets following two-week BQ treatment of CFPAC-1 (left) or S2-013 (right) cells at the indicated doses **D)** Heatmap showing log2 fold change mRNA expression of APP genes in CFPAC-1 cells treated with BQ for indicated dose and duration. **E)** Heatmap showing log2 fold change mRNA expression for APP genes in A375 melanoma cells treated with the DHODH inhibitor teriflunomide (25μM) for indicated durations, data extracted from [38]. **F)** RT-qPCR quantification of *HLA-A, HLA-B*, and *HLA-C* mRNA levels in cancer cell lines after 24-hour BQ treatment. Numbers represent fold change relative to vehicle control for each cell line. Data are representative of at least 3 independent experiments. *HLA-B* was not detectable in MiaPaCa2 cells. **G-H)** Flow cytometry analysis of cell surface MHC-I in live CFPAC-1 (G) or B16F10 (H) cells following 10-day treatment with BQ (250nM for CFPAC-1 and 10μM for B16F10). **I-J)** LC-MS/MS metabolomics quantification of de novo pyrimidine pathway metabolites in CFPAC-1 (I) or B16F10 (J) cells following 8-hour BQ treatment at indicated doses. Data represent mean +/-SEM of four (CFPAC-1) or six (B16F10) biological replicates. # indicates p < 0.0001 by two-way ANOVA with Bonferonni's post-comparison test.

## BQ-mediated APP induction depends on pyrimidine nucleotide depletion

To confirm that BQ-or teriflunomide-mediated APP induction was specifically caused by DHODH inhibition (i.e., on-target effect), we asked whether the effect could be reversed by restoring pyrimidine nucleotides. As we previously observed [37], media supplementation with uridine rescued cell viability (**Fig 2A**) and pyrimidine levels (**Fig 2B**) following BQ treatment and partially rescued viability following teriflunomide treatment (Fig S2A). Uridine supplementation likewise blocked mRNA induction of MHC-I transcripts (*H2-Db*, *H2-Kb*, and *B2m*), as well as *Nlrc5* (a major MHC-I transcriptional coactivator) and *Tap1* (required for peptide import into the ER, a key step in MHC-I antigen presentation) by BQ (**Fig 2C**) or teriflunomide (Fig S2B), while uridine alone had no effect (Fig S2C). This same phenotype was observed in HCT116 human colorectal cancer cells (Fig S2D). Concordantly, cell surface MHC-I upregulation by BQ or teriflunomide (24-hour treatment) was abrogated by uridine supplementation (**Fig 2D**), while uridine alone again had no effect (Fig S2E). These results demonstrate that DHODH inhibitor-mediated APP induction is caused by pyrimidine nucleotide depletion.

To further validate this finding, we assessed MHC-I heavy chain mRNA levels in S2-013 cells with DHODH deletion (sgDHODH). We have previously demonstrated that these cells require exogenous uridine for viability and experience profound pyrimidine depletion (>95% depletion of UTP and CTP) after 8-hour incubation in nucleoside-free media [37]. After growing these cells with supplemented uridine (1 mM), we withdrew exogenous nucleosides by changing to new media containing 10% dialyzed FBS. After 72-hour exposure to nucleoside-free media, sgDHODH cells upregulated *HLA-A*, *HLA-B*, and *HLA-C*, and this was reversed by adding back uridine (**Fig 2E**). Importantly, treatment with BQ did not further increase MHC-I mRNA expression (**Fig 2E**, compare blue and red bars). Together with our other data, these results indicate that BQ-mediated APP induction is an on-target phenomenon with respect to DHODH inhibition.

Since uridine addback rescued BQ- and teriflunomide-mediated loss of viability (**Fig 2A**, S2A), we queried whether BQ-mediated APP induction was caused by pyrimidine depletion *per se*, or if it was the result of some nonspecific downstream consequence of pyrimidine starvation, such as DNA damage or loss of cell viability. To address this, we screened a panel of genotoxic chemotherapy agents and small molecule inhibitors for their ability to induce APP genes following 72-hour exposure at previously determined cytotoxic doses in CFPAC-1 cells (**Fig 2F**). Besides interferon gamma (a positive control), BQ, teriflunomide, and GSK983 (another DHODH inhibitor), the only agent that induced APP gene transcription in this assay was mycophenolate, a clinically approved inhibitor of the *de novo* GTP synthesis enzymes inosine monophosphate dehydrogenase 1 and 2 (IMPDH1/2). The effect of mycophenolate on APP gene expression was subsequently validated in B16F10 cells (Fig S2F), demonstrating that either purine or pyrimidine nucleotide depletion can induce cancer cell APP mRNA expression *in vitro*.

The other drugs screened included nucleotide synthesis inhibitors (5-fluorouracil, methotrexate, gemcitabine, and hydroxyurea), DNA damage inducers (oxaliplatin, irinotecan, and cytarabine), a microtubule targeting drug (paclitaxel), a DNA methylation inhibitor (azacytidine), and other small molecule inhibitors (**Fig 2F**). While we cannot rule out the possibility that these agents induce APP transcription in other cell lines or under other dose/duration conditions, the inertness of these compounds (with respect to APP gene expression) in our screen suggests that BQ-mediated APP induction in CFPAC-1 cells is not a general phenomenon that occurs downstream of DNA damage or some other response to therapy-induced stress.

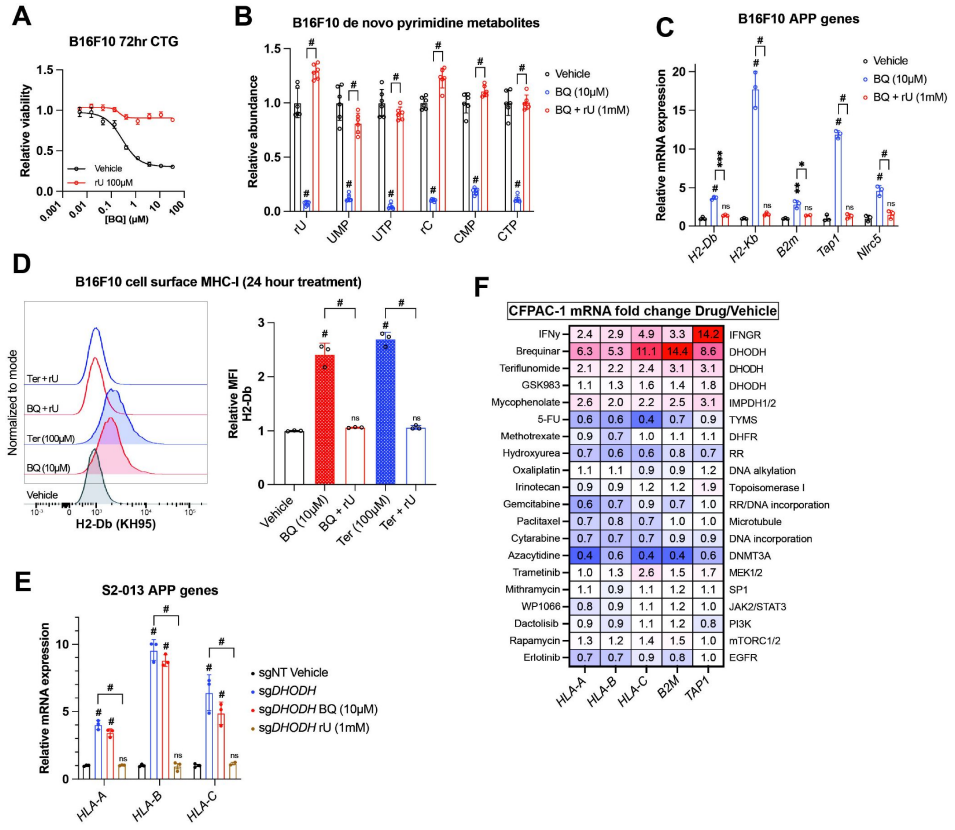


## Figure 2

### BQ-mediated APP induction requires pyrimidine nucleotide depletion.

**A)** Dose-response cell viability experiment in B16F10 cells treated with BQ +/-uridine (100μM) for 72 hours. Data represent mean +/-SEM of three biological replicates. One representative result of three independent experiments is shown. **B)** Quantification of pyrimidine metabolites following 24-hour treatment of B16F10 cells with vehicle, BQ (10μM), or BQ + uridine (1mM). Data represent mean +/-SEM of six biological replicates. # indicates $p < 0.0001$ by two-way ANOVA with Bonferonni post-comparison test. **C)** RT-qPCR of indicated genes in B16F10 cells following 24-hour treatment with BQ (10μM) +/-uridine (1mM). Data represent mean +/-SD of three technical replicates. One representative result of three independent experiments is shown. **D)** Left: flow cytometry analysis of cell surface MHC-I (H2-Db) on live B16F10 cells following 24-hour treatment with indicated agents (BQ 10μM, teriflunomide 100μM, uridine 1mM). Right: quantification of H2-Db mean fluorescence intensity normalized to vehicle control. Data represent mean +/-SEM of three independent experiments. # indicates $p < 0.0001$ with two-way ANOVA with Bonferroni post-comparison test. **E)** RT-qPCR analysis of indicated genes in S2-013 cells with DHODH knockout (sgDHODH) or non-targeting control vector (sgNT) treated with indicated agents for 72 hours. Data represent mean +/-SD of four determinations. One representative result of three independent experiments is shown. **F)** RT-qPCR analysis of indicated genes in CFPAC-1 cells following 72-hour treatment with indicated agents. Numbers in the heatmap represent mean fold change versus vehicle control with four determinations.

## BQ-mediated APP induction does not depend on canonical APP transcriptional regulators

To elucidate the molecular pathway leading to APP induction downstream of pyrimidine depletion, we extended our findings to HEK-293T cells, which also display rapid (within 4 hours) transcriptional induction of MHC-I upon BQ treatment (Fig S3A). Reasoning that the mechanism of this phenomenon in HEK-293T cells is less likely to involve idiosyncratic genetic aberrations than in cancer cell lines, we chose to conduct our initial mechanistic studies in this system and then extend our findings to cancer cell lines if possible.

We used a candidate-based chemical biology screening approach to ask if drugs targeting suspected pathways might block BQ-mediated APP induction in HEK-293T cells. We first interrogated pathways that are known to control MHC/APP expression, including IFN-JAK-STAT [39], NF-κB [27,40], and cGAS-STING-TBK1 [41]. Neither ruxolitinib (a JAK1/2 inhibitor with activity against STAT3) nor GSK8612 (a TBK1 inhibitor) [42], nor TPCA-1 (an IKK2 inhibitor) [43] abrogated BQ-mediated APP induction (**Fig 3A**), despite blocking APP induction downstream of poly(dA:dT) and interferon gamma (Fig S3B) as expected. This indicates that these canonical regulators of MHC/APP expression are dispensable for APP induction downstream of DHODH inhibition.

Interestingly, the IKK2 inhibitor BMS-345541 [44] mostly abrogated BQ-mediated APP induction (**Fig 3A**). BMS-345541 effectively blocked BQ- and Ter-mediated APP induction at concentrations of 10 μM and 40 μM, but not 2.5 μM (**Fig 3B**). The effect of BMS-345541 was confirmed in B16F10 (**Fig 3C**), CFPAC-1 (**Fig 3D**), and HCT116 (**Fig 3E**) cells. Furthermore, BQ treatment (24 hours) of HCT116 cells caused increased cell surface expression of MHC-I, which could be reversed by either uridine supplementation or by treatment with BMS-345541; neither uridine nor BMS-345541 alone affected cell surface MHC-I expression (**Fig 3F**).

Given that TPCA-1 (an established IKK2 inhibitor [43]) did not block BQ-mediated APP induction (**Fig 3A**, **3C**), we suspected that this effect of BMS-345541 was independent of IKK2. To test this, we used previously reported MiaPaCa2 cells with CRISPR-Cas9 deletion of *IKK2* (MiaPaCa2-*IKK2*-KO) [45]. Increased APP mRNA expression was observed upon BQ, teriflunomide, or GSK983 treatment (all DHODH inhibitors) of either wild-type or *IKK2*-KO MiaPaCa2 cells (Fig S3C). However, while TNF-alpha stimulation induced APP and *CCL5* (a canonical NF-κB target gene downstream of TNF-alpha [46]) expression in wild-type cells, this was not observed in *IKK2*-KO cells, as expected (Fig S3C, far right). Finally, BQ-mediated APP induction in *IKK2*-KO cells was significantly reversed with concurrent BMS-345541 treatment (**Fig 3G**). Together, these results demonstrate that IKK2 is dispensable for BQ-mediated APP induction and that the observed reversal effect of BMS-345541 is independent of IKK2.

## Nucleotide starvation induces APP transcription in a P-TEFb-dependent manner

To further investigate the mechanism by which BMS-345541 blocks APP induction downstream of pyrimidine starvation, we leveraged publicly available data on the target profile of BMS-345541 and other agents tested in the cell-free KINOMEscan assay [47]. BMS-345541 reproducibly bound more than 20 kinases, with dissociation constants ($k_d$) ranging from 130-8100 nM (**Fig 4A**). We prioritized potential targets with a $k_d$ in the low micromolar range, given that 2.5 μM BMS-345541 did not block BQ-mediated APP induction in our previous experiments, and the effect seemed to be maximal at 10 μM, with no significant increase in the magnitude of the effect between 10 μM and 40 μM (**Fig 3B**). Additionally, we prioritized targets that were >50% inhibited with 10 μM BMS-345541 treatment. These two conditions correspond to the upper left quadrant of **Fig 4A**.

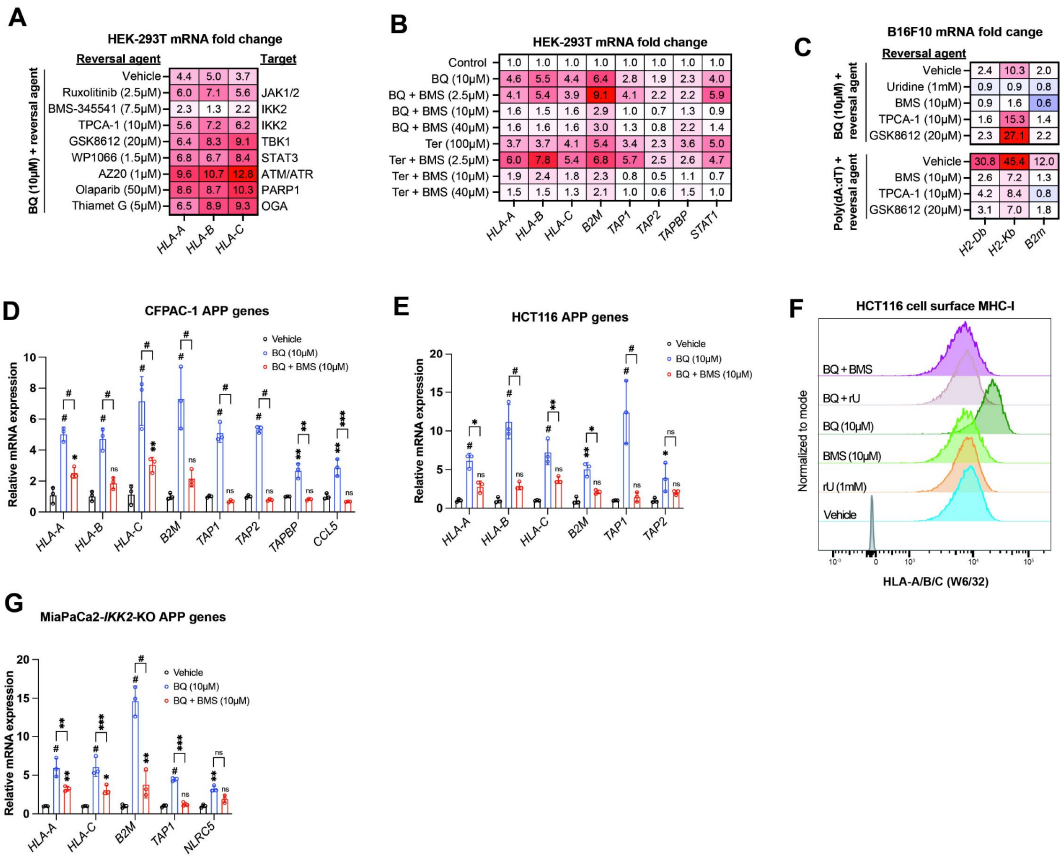


## Figure 3

### IKK2 inhibitor BMS-345541 abrogates BQ-mediated APP induction in an IKK2-independent manner.

**A-B)** HEK-293T cells were treated with indicated agents for 24 hours and then subjected to RT-qPCR analysis for indicated genes. Numbers in the heatmap represent mean of four determinations. **C-E, G)** B16F10 (C), CFPAC-1 (D), HCT116 (E) or MiaPaCa2-IKK2-KO (G) cells were treated with indicated agents for 24 hours and subjected to RT-qPCR analysis of indicated genes. Data in D,E, and G represent mean +/-SD of three independent experiments. * indicates $p < 0.05$, ** $p < 0.01$, *** $p < 0.001$, and # $p < 0.0001$ with two-way ANOVA with Bonferroni post-comparison test. For C, numbers in the heatmap represent mean fold change versus vehicle with three determinations. Representative result of three independent experiments is shown. **F)** Flow cytometry analysis of cell surface MHC-I in HCT116 cells treated with indicated agents for 24 hours.

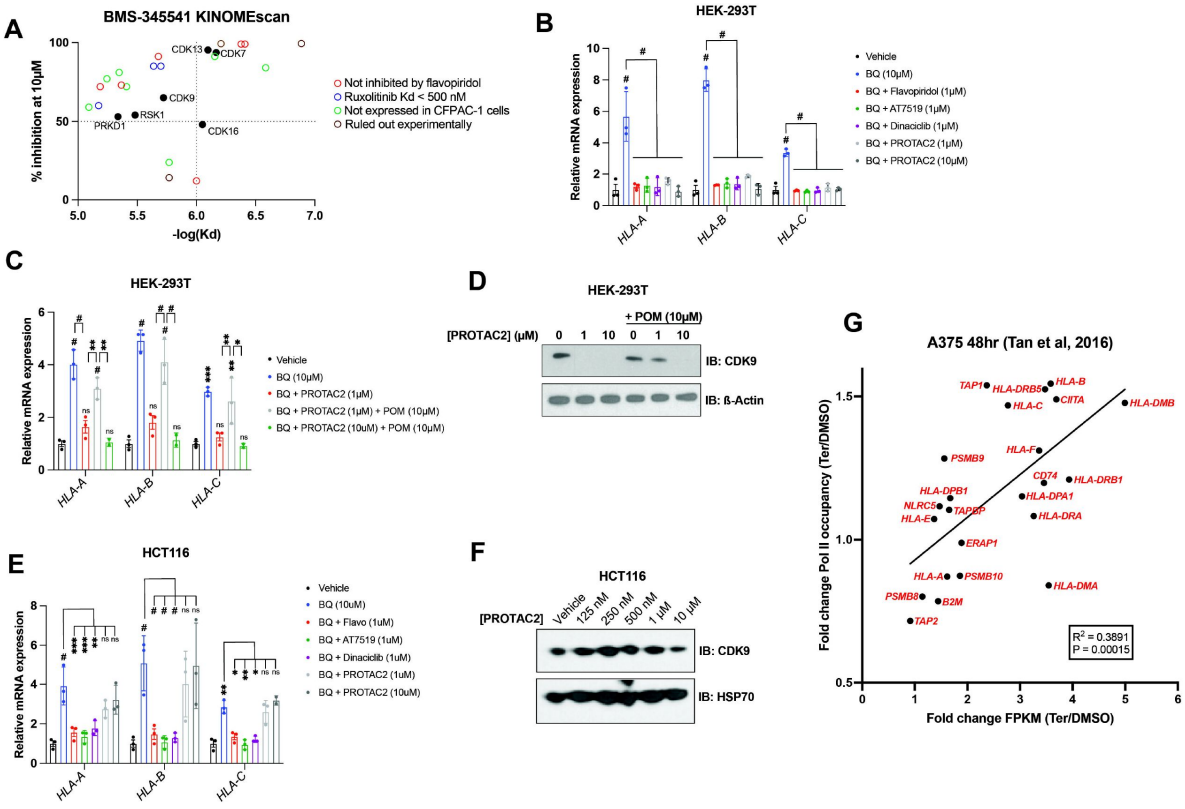


## Figure 4

### P-TEFb inhibitor flavopiridol abrogates APP induction downstream of nucleotide depletion.

**A)** Plot of percent inhibition (10μM treatment) vs -log(dissociation constant) for kinases bound by BMS-345541 in KINOMEscan assays [47]. Each data point represents an individual kinase. **B-C)** RT-qPCR analysis for indicated genes in HEK-293T cells treated with indicated agents for 24 hours. Data represent mean +/-SD of three independent experiments. * indicates $p < 0.05$, ** indicates $p < 0.01$, *** indicates $p < 0.001$, and # indicates $p < 0.0001$ by two-way ANOVA with Bonferonni's post-comparison test **D)** Western blot analysis for CDK9 performed on HEK-293T cells treated with CDK9-targeted PROTAC (PROTAC2) and/or pomalidomide (POM) for 24 hours. Beta actin was used as a loading control. **E)** RT-qPCR analysis of indicated genes after 24-hour treatment with indicated agents. Data represent mean +/-SD of three independent experiments. **F)** Western blot analysis for CDK9 performed on HCT116 cells treated with the indicated concentrations of PROTAC2 for 24 hours. Heat shock protein 70 (HSP70) was used as a loading control **G)** Linear regression analysis of fold change (teriflunomide/DMSO) in Pol II occupancy (assessed by ChIP-seq) versus fold change (teriflunomide/DMSO) in mRNA abundance (assessed by RNAseq) following 48-hour treatment of A375 cells with teriflunomide or DMSO vehicle control; data derived from [38].

One potential target that met the selection criteria was CDK9, which together with cyclin T1 or T2 forms positive transcription elongation factor B (P-TEFb). P-TEFb is required for the release of promoter-proximal paused RNA polymerase II (Pol II) into productive elongation and therefore is essential for Pol II transcription from paused promoters [48,49]. The potent P-TEFb inhibitor flavopiridol [50] phenocopied BMS-345541 in our assays, as it blocked APP induction downstream of DHODH, IMPDH1/2 (by mycophenolate), or CTP synthase (by 3-deazauridine [51]) inhibition (Fig S4A). This suggests that APP induction downstream of nucleotide starvation requires P-TEFb-mediated paused Pol II release. It also suggests that the BMS-345541 effect of reversing BQ-induced APP upregulation is due to P-TEFb inhibition.

Within the list of kinases bound by BMS-345541 (**Fig 4A**) we eliminated those that were a) not expressed by CFPAC-1 cells in our RNA-seq data, b) not bound by flavopiridol in KINOMEscan data, or c) bound by ruxolitinib in KINOMEscan data with Kd < 500 nM (as 2.5 μM ruxolitinib failed to reverse BQ-mediated APP induction (**Fig 3A**)). Five candidates (besides CDK9) remained that were bound by both BMS-345541 and flavopiridol in KINOMEscan assays. Of these, three are CDKs known to play a role in transcription (CDK7, CDK13, and CDK16). Inhibition of any of these CDKs could theoretically account for the observed effects of flavopiridol and BMS-345541. However, previous studies suggest that flavopiridol inhibition of these CDKs in vivo is much less efficient than in cell-free assays because it is competitive with ATP (and thus less efficient in living cells where the ATP concentration is in the 1-10 mM range, which is much higher than in cell-free assay conditions), while its inhibition of P-TEFb is not affected by ATP concentration [50]. Furthermore, flavopiridol and the CDK7 inhibitor THZ1 have very different (and mutually exclusive) effects on transcriptional processes [52], arguing against CDK7 inhibition as the mechanism of flavopiridol's effect.

To further probe whether the observed effect of flavopiridol was due to CDK9 inhibition, we tested two other CDK9 inhibitors (AT7519 and dinaciclib). Both CDK9 inhibitors phenocopied flavopiridol in our assays (**Fig 4B**). Furthermore, a previously characterized CDK9-targeted proteolysis targeting chimera (PROTAC), termed PROTAC2 [53], had the same effect (**Fig 4B**). PROTAC2 consists of a CDK9-binding aminopyrazole warhead conjugated to pomalidomide, which recruits the E3 ubiquitin ligase Cereblon (*CRBN*). Cereblon in turn ubiquitinates CDK9, resulting in its proteasomal degradation. Co-treatment of HEK-293 cells with PROTAC2 and pomalidomide prevents PROTAC2-mediated CDK9 degradation, as free pomalidomide competes with PROTAC2 for Cereblon binding [53]. We observed that PROTAC2 (1 μM) blocked BQ-mediated APP induction, and this effect was reversed by co-treatment with 10-fold excess pomalidomide (10 μM); however, when we increased the concentration of PROTAC2 to 10 μM (so that PROTAC2 and pomalidomide concentrations were equal), pomalidomide no longer had this effect (**Fig 4C**). Consistently, immunoblot analysis showed that 10 μM pomalidomide prevents CDK9 degradation upon 1 μM but not 10 μM PROTAC2 treatment (**Fig 4D**). When we repeated the experiment shown in **Fig 4B** with HCT116 cells, we found that all CKD9 inhibitors reversed BQ-mediated APP induction, but PROTAC2 did not (**Fig 4E**). Concordantly, immunoblot analysis showed that PROTAC2 did not cause CDK9 depletion in HCT116 cells treated in parallel (**Fig 4F**).

Taken together, these results demonstrate that CDK9 degradation is necessary for the reversal effect of PROTAC2 and that CDK9 is required for BQ-mediated APP induction.

The dependence of BQ-mediated APP induction on CDK9 strongly suggests that nucleotide starvation enforces nascent transcription of APP genes, as opposed to increased mRNA stability. This is further supported by the rapid buildup of APP transcripts following DHODH inhibitor treatment (within 4 hours, Fig S3A). Additionally, ChIP-seq analysis of global Pol II occupancy following 48-hour teriflunomide treatment in A375 cells [38] shows increased Pol II occupancy across many APP genes, and fold change in Pol II occupancy significantly correlated with fold

change in mRNA expression under the same conditions (**Fig 4G**). Overall, these results show that nucleotide starvation induces an antigen presentation gene expression program that is independent of canonical APP regulators but depends on CDK9/P-TEFb.

## BQ suppresses tumor growth, induces MHC-I expression, and increases immunotherapy efficacy in a syngeneic melanoma model

Enforced MHC-I upregulation by various interventions can facilitate anticancer immunity and enhance the efficacy of immune checkpoint blockade (ICB) by antibodies directed at PD-(L)1 and/or CTLA-4 [24-27]. Moreover, high MHC-I expression has been proposed as a predictor of ICB response [28-31], and high expression of MHC-I and other APP genes, including *NLRC5* and *TAP1*, correlates with better survival in patients with melanoma (Fig S5A), for whom ICB is a first-line therapy. Therefore, we asked if BQ could improve anticancer immunity in the B16F10 melanoma immunocompetent mouse model, which is typically refractory to dual ICB (i.e., anti-PD-1 plus anti-CTLA-4) [54].

BQ (10 mg/kg daily IP injection) markedly suppressed tumor growth and led to reduced tumor burden (**Fig 5A-B**). Historically, the lead tool compound that was ultimately modified to BQ (called NSC 339768) was prioritized in part based on its activity against B16 melanoma [55]; however, to our knowledge, this is the first direct demonstration of BQ activity in this model system. Consistent with our *in vitro* metabolomics data (**Fig 1I-J**, S1B), BQ treatment caused marked buildup of metabolites upstream of DHODH and depletion of downstream pyrimidine nucleotide species in B16F10 tumors (**Fig 5C**), confirming target engagement *in vivo*. Metabolomics analysis of BQ- and vehicle-treated tumors separated in principal component analysis (Fig S5B) and unsupervised hierarchical clustering (Fig S5C), confirming the perturbation of tumor metabolism following DHODH inhibition.

BQ-treated B16F10 tumors showed increased mRNA expression of MHC-I (*H2-Db* and *H2-Kb*) and *Nlrc5* (**Fig 5D**). We thus addressed whether BQ could augment the efficacy of dual ICB (anti-CTLA-4 plus anti-PD-1) with the knowledge that enforced MHC-I antigen presentation has also been shown to boost the effect of ICB [24,26,27]. While BQ is not an approved medication, two FDA-approved low potency DHODH inhibitors (leflunomide, teriflunomide) are effective in treating autoimmune conditions such as rheumatoid arthritis and multiple sclerosis and act to decrease the activity of auto-reactive T-lymphocytes [56-58]. It was possible that BQ treatment may actually impair the effectiveness of ICB by inhibiting T-lymphocytes despite augmented cancer cell antigen presentation. We, therefore, tested both concurrent, upfront administration of BQ plus dual ICB and sequential administration of BQ followed by dual ICB (Fig S5D).

Similar to its impressive activity in our first experiment (**Fig 5A-B**), BQ monotherapy conferred marked survival benefit. This was significantly enhanced by subsequent dual ICB, while dual ICB alone conferred only marginally prolonged survival, and concurrent BQ plus dual ICB did not significantly improve survival versus BQ monotherapy (**Fig 5E**). This suggests that sequential (rather than concurrent) administration of DHODH inhibitor and ICB may be superior. Hypotheses that may explain these findings include: a) Concurrent BQ dampens the initial anticancer immune response generated by dual ICB, or b) cancer cell MHC-I and related genes are not maximally upregulated at the time of ICB administration with concurrent treatment. Taken together, these results show that BQ causes pyrimidine nucleotide depletion, MHC-I and APP gene transcriptional upregulation, and additive survival benefit with dual ICB in a highly aggressive and ICB-refractory mouse melanoma model.

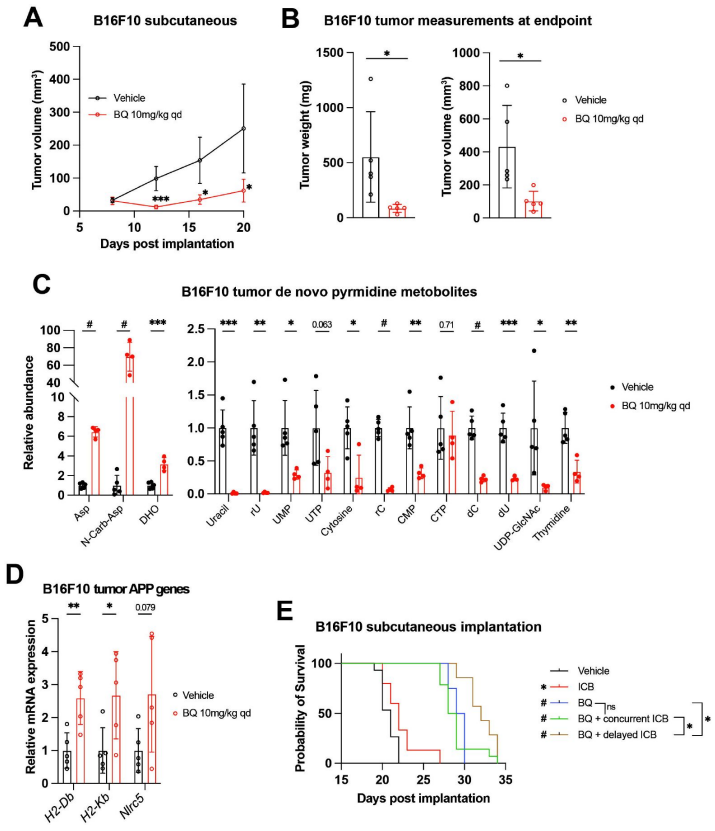


## Figure 5

### BQ inhibits tumor growth, increases tumor MHC-I, and enhances immune checkpoint blockade efficacy in B16F10 murine melanoma model.

**A-D)** B16F10 cells were injected subcutaneously into syngeneic hosts and mice were treated with brequinar (BQ; 10mg/kg IP daily) or vehicle control starting at day 7 post implantation. **A)** Longitudinal measurement of B16F10 subcutaneous tumors with BQ (10mg/kg IP daily) or vehicle treatment. **B)** Weight (left) and volume (right) of tumors at necropsy. **C)** Quantification of metabolites from B16F10 tumors harvested at necropsy. **D)** RT-qPCR analysis of APP genes from tumors harvested at necropsy. For (A-D), data represent mean +/-SD of n = 5 mice per group (n = 4 for BQ group in C). * indicates $p < 0.05$, ** indicates $p < 0.01$, *** indicates $p < 0.001$, and # indicates $p < 0.0001$ by unpaired t-test. **E)** Kaplan-Meier survival analysis for mice implanted with B16F10 tumors as in (A-D) and treated with indicated regimens; see Fig S5D for treatment timeline. * indicates $p < 0.05$, # $p < 0.0001$ by Mantel-Cox logrank test. For vehicle, immune checkpoint blockade (ICB; Anti-CTLA-4 and anti-PD-1; 100µg/mouse each, IP twice per week), and BQ (10mg/kg IP daily) + concurrent ICB, n = 15. For BQ, n = 7. For BQ + delayed ICB, n = 8.

## Discussion

Our results demonstrate that pyrimidine nucleotide depletion by DHODH inhibition causes increased expression of APP genes and increased antigen presentation via MHC-I across a diverse panel of cancer cell lines (**Fig 1**). This effect of BQ and teriflunomide is strictly dependent on pyrimidine nucleotide depletion, as it was abrogated by restoration of pyrimidine levels with exogenous uridine (**Fig 2B-D** and Fig S2B-E). Furthermore, genetic deletion of *DHODH* recapitulated this effect, and treatment of DHODH knockout cells with BQ did not further increase MHC-I mRNA expression (**Fig 2E**). Our inhibitor reversal studies determined that BQ-mediated APP induction is independent of several canonical APP regulatory pathways, including IFN-JAK-STAT, cGAS-STING-TBK1, and NF-κB (**Fig 3** and Fig S3). We showed that this effect relies on P-TEFb-mediated release of Pol II from promoter-proximal paused state to productive elongation (**Fig 4**). These findings were extended to inhibition of IMPDH (which depletes cellular GTP) and CTPS (which depletes cellular CTP), as these effects were also reversible with P-TEFb inhibition (Fig S4A). This suggests that pharmacologic depletion of these nucleotide species also triggers APP upregulation in a P-TEFb-dependent manner.

Since T-cell recognition of antigens via MHC-I is required for T-cell-mediated elimination of cancer cells or virus-infected cells, these results have important implications for the development of nucleotide synthesis inhibitors as anticancer/antiviral therapies. We provide proof of concept evidence that pretreatment with DHODH inhibitors can improve the efficacy of immune checkpoint blockade in a highly aggressive and ICB-refractory mouse melanoma model (**Fig 5** and Fig S5). Because BQ-mediated APP induction does not require interferon signaling, this strategy may have particular relevance for clinical scenarios in which tumor antigen presentation is dampened by the loss or silencing of cancer cell interferon signaling, which has been demonstrated to confer both intrinsic [59] and acquired [23] ICB resistance in human melanoma patients.

Emerging evidence suggests that cancer cell MHC-I expression predicts favorable response to ICB, and several recent studies have shown that enforced cancer cell MHC-I expression enhances anticancer immunity and ICB efficacy in various mouse models. Accordingly, functional genomic screens for regulators of cancer cell MHC-I expression have recently been undertaken, and these efforts have revealed novel molecular targets to induce cancer cell APP activity [27,60]. Agents shown to increase cancer cell antigen presentation include hydroxychloroquine (by autophagy inhibition) [24], poly(I:C) (by NF-κB activation downstream of dsRNA sensing) [26], SMAC mimetics (by NF-κB activation) [27], CDK4/6 inhibitors (by activation of endogenous genomic retroviral elements) [25], and others. It is very likely that many other anticancer drugs perturb cancer cell antigen presentation and/or have other immunomodulatory properties in addition to their cell-intrinsic antiproliferative activity [61], and this area requires further scrutiny. In this study, we identified DHODH inhibition as a powerful inducer of antigen presentation and MHC-I expression in diverse cancer cell lines and in HEK-293T cells.

Previous studies have linked pyrimidine depletion with upregulation of innate immunity and interferon-stimulated genes [33,34], and this was confirmed by our transcriptomic profiling experiments (**Fig 1B-C**). Multiple mechanistic explanations for these observations have been suggested. Lucas-Hourani et al. proposed that interferon-stimulated gene expression requires the DNA damage checkpoint kinase ATM [33], while Sprenger et al. conclude that pyrimidine depletion causes accumulation of mitochondrial DNA in the cytosol, which is sensed by the cGAS-STING-TBK1 pathway to promote innate immunity [34]. In our models, neither ATM/ATR nor TBK1 inhibition blocked BQ-mediated APP induction (**Fig 4A**). It is possible that pyrimidine nucleotide shortage leads to APP induction by multiple redundant mechanisms, any of which may predominate based on the cellular context. We speculate that cells may have evolved multiple

means of sensing acute pyrimidine shortage as a way to detect viral infection or malignant transformation, as both viral replication and uncontrolled cell proliferation avidly consume nucleotides.

Our focused chemical screen for MHC-I inducers (**Fig 2F**) identified the approved IMPDH1/2 inhibitor mycophenolate, which was subsequently validated in multiple other cell types (Fig S2D, S4A). This is consistent with a recent study in which IMPDH inhibition was shown to enhance ICB efficacy by favorably altering the MHC-I peptide repertoire and increasing immunoproteasome expression [62]. However, in this study, the cancer cells were pretreated with IMPDH inhibitor before implantation into syngeneic hosts, and so possible countervailing immunosuppression by systemic IMPDH inhibitor treatment was not addressed [62]. Our *in vivo* results (**Fig 5F**) highlight the importance of timing/sequence when administering immunotherapy in combination with nucleotide synthesis inhibitors and suggest that upfront BQ followed by ICB may be superior to concurrent administration.

Thymidylate synthase inhibition was recently shown to induce MHC-I in a model of diffuse large B cell lymphoma [60]. The failure of thymidylate synthase inhibitors 5-fluorouracil and methotrexate to induce MHC-I in our screen (**Fig 2F**) may be attributable to cell line differences (PDAC vs DLBCL), dose/duration considerations, or the use of different thymidylate synthase inhibitors than in their study (which used pemetrexed and raltitrexed). Thus, it appears that the abundance of multiple nucleotide species can exert context-dependent influence on MHC and APP gene expression, and key details of this relationship remain to be elucidated.

Overall, our study establishes P-TEFb and Pol II elongation control as a mechanistic link between nucleotide depletion and APP induction. We provide proof of concept evidence for combinatorial benefit of DHODH inhibition and immune checkpoint blockade in an aggressive and poorly immunogenic mouse model of melanoma. A deeper understanding of metabolic control of antigen presentation will enable rational therapy development for cancer and viral infection.

# Materials and Methods

## Cell culture and cell lines

The S2-013 cell line is a clonal derivative of the Suit2 cell line and was a kind gift from the Tony Hollingsworth laboratory at the University of Nebraska Medical Center. The MiaPaCa2 *IKK2*-KO and parental wild-type MiaPaCa2 cell lines were a kind gift from the Amar Natarajan laboratory at the University of Nebraska Medical Center. All other cell lines in this study were obtained from American Type Culture Collection (Manassas, VA, USA). All human cell lines were authenticated by STR profiling by the Genetics Core at the University of Arizona. Cells were routinely (at the time of initial revival from liquid nitrogen storage and at least every 6 months) determined to be free of mycoplasma contamination by PCR-based methods. Cells were cultured in Dulbecco's modified Eagle medium (Sigma-Aldrich, St Louis, MO, USA) supplemented with 50 IU/mL penicillin, 50[µg/mL streptomycin, and incubated at 37[°C in a humidified incubator with 5% $CO_2$. Cells were maintained at 10% fetal bovine serum (FBS). Upon reaching 70–80% confluency, cells were passaged by washing with phosphate-buffered saline (PBS) before adding 0.25% trypsin (Caisson Labs, Smithfield, UT, USA) and plating at 25% confluency.

## Drug treatment of cultured cells for RT-qPCR and flow cytometry experiments

Drug treatment dose and duration are indicated for each experiment. A table of manufacturer and catalog number for each agent described can be found in Supplementary Table 1. For stimulation with poly(dA:dT), 2µg of poly(dA:dT) and 2µl of Lipofectamine2000 (Invitrogen #11668027) were

incubated in 400µl Opti-MEM (Gibco #11058021) for 30 minutes at room temperature and then added to cells in 2ml final volume of complete media.

## Cell viability assays

Cells were seeded in 96 well plates (1000 cells per well in 90µl media) and allowed to equilibrate overnight. Cells were then treated with indicated compounds (final volume 100µl) for 72 hours, and viability was assessed by CellTiter-Glo assay (Promega, Madison, WI). Luminescence values for each condition were normalized to the average luminescence of the vehicle-treated control replicates. Experiments were performed at least three times using biological triplicates for each condition. Dose-response curves were fit to nonlinear regression models using Prism9 software.

## Liquid chromatography – tandem mass spectrometry-based metabolomics analysis

For in vitro metabolomics experiments, 5 x $10^5$ cells were seeded in 6-well plates and allowed to equilibrate overnight. At the start of each assay, the cell culture media was changed, and fresh media with desired conditions was added (to eliminate metabolite depletion from overnight equilibration as a confounding variable). Following 8-hour treatment of cancer cell lines with BQ (or in the case of **Fig 2B**, 24-hour treatment with BQ +/-100µM uridine), polar metabolites were extracted and quantified as previously described [63]. For B16F10 tumor metabolomics, subcutaneous tumors were harvested at necropsy and immediately snap frozen in liquid nitrogen and stored at -80 °C. Tumors were subsequently ground into fine powder in liquid nitrogen using a mortar and pestle, and metabolites were extracted using the same method as for cultured cells. Peak areas were normalized to the mass of tumor tissue that was input.

Datasets were processed using Skyline (MacCoss Lab Software), and Metaboanalyst5.0 web tool was used to generate principal component analysis and heatmap visualizations of resulting datasets. Raw LC-MS/MS data and R-command history for Metaboanalyst analysis are available upon request. Relative metabolite abundances were normalized to the average peak area of the experimental control group and were compared using two-way ANOVA with Bonferonni's post-test correction for multiple comparisons. $P < 0.05$ was considered significant.

## Mice studies

All procedures were approved by the Institutional Animal Care and Use Committee (IACUC) at the University of Nebraska Medical Center. For tumor xenograft studies, $10^4$ B16F10 cells in a 1:1 vol/vol ratio (100µl final volume) with Matrigel were injected subcutaneously into the right flank of 10-week-old female C57BL/6J mice (Jackson labs). Tumors of live mice were serially measured in two dimensions using digital calipers, and tumor volume for **Fig 5A** was calculated as (0.5L x $W^2$), where L is the long dimension and W is the short dimension. For **Fig 5B-C**, tumors were harvested at necropsy, weighed on an analytical balance (for **Fig 5B**), and measured in three perpendicular dimensions by calipers to generate volume measurements for **Fig 5C**, which were calculated as (dimension 1 x dimension 2 x dimension 3).

For survival experiments (**Fig 5F**), mice were monitored daily for signs of euthanasia criteria or actual demise. When tumor volume reached 2000$cm^3$ as determined by the above formula for live mice (0.5L x $W^2$), mice were sacrificed according to protocol euthanasia criteria.

Brequinar was obtained from Clear Creek Bio and dissolved in 0.9% NaCl. For both endpoint and survival studies, BQ (10mg/kg) or vehicle solvent (0.9% NaCl) was injected intraperitoneally daily. Anti-CTLA-4 and anti-PD-1 antibodies, as well as their respective isotype controls, were obtained from BioXCell. Antibodies were dosed at 100µg/mouse IP twice per week.

## RNA sequencing and gene set enrichment analysis

For RNA sequencing experiments, S2-013 or CFPAC-1 cells were treated with brequinar for the indicated dose and duration (**Fig 1** and S1). For two-week drug treatment experiments, cells were passaged every 3 days and 5 x $10^5$ cells were reseeded in a new 10cm tissue culture dish. RNA was isolated using RNEasy Mini kit (Qiagen, catalog number 74104).

Samples were processed by BGI Genomics (San Jose, California, USA) according to their proprietary method. Briefly, RNA quality check was performed using Agilent 2100 Bioanalyzer. Poly-A-containing mRNA was isolated using magnetic beads and then fragmented using divalent cations under elevated temperature. cDNA synthesis was performed using reverse transcriptase and RNase H. Adapter sequences were then ligated onto cDNA fragments, purified, enriched by PCR, quantified by Qubit, and pooled to generate the final library. Libraries were then sequenced using the BGI DNBseq platform. Reads mapped to rRNA, low quality reads, and reads with adaptors were removed. The resulting clean reads were mapped to the reference genome (hg19_UCSC_20180115) using HISAT2 program (*http://www.ccb.jhu.edu/software/hisat/index.shtml*) and converted to fragments for kilobase per million mapped reads (FPKM).

Fold change FPKM (brequinar/vehicle control) values for all expressed genes (FPKM > 1) were subjected to gene set enrichment analysis [36] with GSEA prerank using HALLMARK and KEGG genes sets from the Molecular Signatures Database (MSigDB) as previously described [64]. Gene sets positive enriched with FDR q < 0.25 are shown in **Fig 1B**.

## Real time quantitative PCR analysis for mRNA expression

For in vitro RT-qPCR experiments, RNA was harvested using Trizol reagent (Thermo Fisher Scientific, Waltham, MA, USA) according to manufacturer's instructions. For tumor RT-qPCR, tumors were crushed with mortar and pestle in liquid nitrogen, and Trizol was used to extract RNA from the resulting powder, just as for cultured cells. cDNA synthesis was performed (1µg RNA input) using BioRad (Hercules, CA, USA) iScript cDNA synthesis kit (catalog number 1708891) according to manufacturer's instructions. For RT-qPCR reactions, 3µl of diluted cDNA, 2µl of primer mix (diluted to a final concentration of 200 nM for forward and reverse primers), and 5µl SYBR green master mix (cat #) were mixed (10µl final volume), and reactions were analyzed using Applied Biosystems QuantStudio5 instrument with previously reported thermocycling parameters [65].

18S rRNA was used as a loading control to generate delta Ct values, and each sample was normalized to the experimental control delta Ct values to generate delta delta Ct values which were converted to fold change by ($2^{\wedge}$-ddCt). For all experiments, *ACTB* (beta-actin) mRNA expression was quantified and used as an additional loading control, and results were concordant regardless of whether 18S or *ACTB* was used for normalization. For **Fig 5E**, each data point represents the average expression value of 4 technical replicates for an individual tumor.

For pairwise comparisons, an unpaired student's t-test was used. For comparisons of 3 or more conditions, a two-way ANOVA with Bonferonni's post-test correction for multiple comparisons was used. P < 0.05 was considered significant. Primer sequences for RT-qPCR reactions are provided in Supplementary Table 2.

## Flow cytometry measurement of cell surface MHC-I

Cells were treated as described and then detached with Accutase (Sigma Aldrich #A6964), washed twice with PBS, stained with fluorescent dye-conjugated antibodies against H2-Db (BioLegend #111508) or HLA-A/B/C (BioLegend #311418, BioLegend #311406) for 30 minutes at 4 °C in PBS, washed once more with PBS, and then resuspended in FACS buffer and subjected to flow cytometry analysis for fluorescence intensity. Aqua live/dead dye (Invitrogen #L34957) or propidium iodide was used to exclude dead cells from the analysis.

## Western blot

Protein isolation from cultured cells and western blotting procedure were described previously [63]. CDK9 antibody was obtained from Cell Signaling Technology (catalog number 2316, clone C12F7), HSP70 antibody was obtained from Cell Signaling Technology (catalog number 4872), and beta-actin antibody was obtained from Santa Cruz Biotechnology (catalog number sc-4778, clone C4). Blots were incubated with primary antibody overnight at 4 °C, washed, incubated with secondary antibody conjugated with horseradish peroxidase for 45 min at room temperature, washed, developed with ECL reagent and visualized by autoradiography using plain film.

## Procurement and analysis of previously published datasets

All datasets reported by Tan and colleagues [38] were obtained from Gene Expression Omnibus, accession numbers GSE68053 and GSE68039. Processed RNA sequencing data for human A375 melanoma cells treated with DMSO vehicle control (GSM1661518, GSM1661518), or teriflunomide (25μM) for 12 hours (GSM1661510, GSM1661511), 24 hours (GSM1661512, GSM1661513), 48 hours (GSM1661514, GSM1661515), or 72 hours (GSM1661516, GSM1661517) was downloaded as an Excel file from GSE68039 (GSE6809_A375.FPKM.xls) and directly analyzed by manual inspection. The two FPKM values for each experimental condition were averaged, and these average values were used to calculate the fold change (teriflunomide/DMSO) values presented in **Figure 1E** and **Figure 4G**.

For chromatin immunoprecitation sequencing (ChIP-seq) datasets (used to generate **Fig 4G**), Fastq files for human A375 melanoma cells treated for 48 hours with DMSO (GSM1661790) or teriflunomide (GSM1661791) for were downloaded from GSE68053, trimmed of adapter sequences at the 3'ends with trim_galore v0.6 (*https://github.com/FelixKrueger/TrimGalore*), and aligned to hg38 using Bowtie (v1.2.3) (ref = *https://genomebiology.biomedcentral.com/articles/10.1186/gb-2009-10-3-r25*) with parameters --minins 18 --maxins 1000 --fr --best --allow-contain. Reads overlapping with the longest transcript of each gene (Genecode v32 and *https://github.com/GeoffSCollins/PolTools/blob/master/PolTools/static/longest_transcript_with_downstream_start_codon.txt*) were counted with BEDtools intersect (v2.27.1). Library size correction factors were calculated separately for the ChIP-seq datasets. The correction factor for a given ChIP-seq sample was computed by dividing the number of mapped reads in that sample by the average number of mapped reads across all ChIP samples (DMSO, A771726). After normalization, the total number of read counts (now corrected for total number of mapped reads per sample) aligned to each gene of interest were used to calculate fold change (teriflunomide/DMSO) in Pol II occupancy values presented in **Figure 4G**.

# Acknowledgements

This work was supported in part by funding from the National Institutes of Health, including R01CA163649 and U54CA274329 to PKS, F30CA265277 to NJM, R21CA251151 to AN, and R35GM126908 to DHP.

# Conflict of Interest Statement

DBS is a co-founder and holds equity in Clear Creek Bio. The other authors declare no competing interests.

# Figure legends

**Figure S1: BQ treatment upregulates APP genes and depletes pyrimidine nucleotides. A)** Heatmap showing log2 fold change mRNA expression of APP genes in S2-013 cells treated with BQ for indicated dose and duration. **B-C)** RT-qPCR quantification of APP genes after two-week BQ treatment of CFPAC-1 (250nM) (B) or B16F10 (10μM) (C) cells. **D-E)** Quantification of pyrimidine metabolites in CFPAC-1 (C) or B16F10 (D) cells treated with BQ for 8 hours at indicated doses. Data represent mean +/-SEM of four (CFPAC-1) or six (B16F10) biological replicates. * indicates $p < 0.05$, ** $p < 0.01$, *** $p < 0.001$, and # $p < 0.0001$ by unpaired t-test (B, C) or two-way ANOVA with Bonferonni's post-comparison test (D, E).

**Figure S2: Uridine rescues B16F10 cells from teriflunomide toxicity but does not alter APP expression by itself. A)** Dose-response cell viability experiment as in **Fig 2A** but with teriflunomide (Ter) instead of BQ. **B)** RT-qPCR analysis of indicated genes following treatment with teriflunomide +/-uridine (1mM) for 24 hours. Data represent mean +/-SEM of three determinations. One representative result of three independent experiments is shown. **C)** RT-qPCR analysis of indicated genes after treatment with vehicle or uridine (1mM) for 24 hours. Data represent mean +/-SEM of four determinations. One representative result of three independent experiments is shown. **D)** RT-qPCR analysis of indicated genes following treatment with BQ (10μM) +/-uridine (1mM) for 24 hours. Data represent mean +/-SD of three independent experiments. **E)** Flow cytometry analysis of cell surface MHC-I (H2-Db) following 24-hour uridine (1mM) treatment. Data represent mean +/-SEM of three independent experiments. **F)** RT-qPCR analysis of indicated genes in B16F10 cells following 24-hour treatment with MPA (5μM). Data represent mean +/-SEM of four determinations. One representative result of three independent experiments is shown.

**Figure S3: A)** RT-qPCR time course analysis for MHC-I genes in HEK-293T cells treated for indicated times with BQ (10μM). Data represent mean +/-SD of four determinations. **B)** RT-qPCR analysis for *Nlrc5* (left) or *Tap1* (right) in B16F10 cells treated for 24 hours with indicated agents. Data represent mean +/-SD of four determinations. # indicates $p < 0.0001$ with two-way ANOVA with Bonferroni post-comparison test. Representative results for one of three independent experiments are shown. **C)** Heatmap indicating RT-qPCR analysis for indicated genes in wild-type or *IKK2*-KO MiaPaCa2 cells treated with indicated agents for 24 hours. Numbers in the heatmap represent mean of four determinations.

**Figure S4: A)** RT-qPCR analysis for indicated genes in HCT116 cells treated with indicated agents in the presence or absence of flavopiridol (1μM). Numbers in the heatmap represent mean of three determinations.

**Figure S5: A)** Overall survival in melanoma patients (SKCM) from the Cancer Genome Atlas (TCGA) with above (indicated in red) and below median (indicated in blue) mRNA expression of indicated genes. **B-C)** Principal component analysis (PCA) plot (B) and unsupervised hierarchical clustering (C) from metabolomics analysis of B16F10 tumors at necropsy (**Fig 5C**). **D)** Treatment regimen of mice from **Fig 5E**.

# References


1 Warburg O. (1956) **On the origin of cancer cells** *Science* **123**:309–314 https://doi.org/10.1126/science.123.3191.309

2 Hanahan D., Weinberg Robert A. (2011) **Hallmarks of Cancer: The Next Generation** *Cell* **144**:646–74 https://doi.org/10.1016/j.cell.2011.02.013

3 Mullen N. J., Singh P. K. (2023) **Nucleotide metabolism: a pan-cancer metabolic dependency** *Nature Reviews Cancer* **23**:275–294 https://doi.org/10.1038/s41568-023-00557-7

4 Wang W., Cui J., Ma H., Lu W., Huang J. (2021) **Targeting Pyrimidine Metabolism in the Era of Precision Cancer Medicine** *Frontiers in Oncology* **11** https://doi.org/10.3389/fonc.2021.684961

5 Shukla S. K., et al. (2017) **MUC1 and HIF-1alpha Signaling Crosstalk Induces Anabolic Glucose Metabolism to Impart Gemcitabine Resistance to Pancreatic Cancer** *Cancer Cell* **32**:71–87 https://doi.org/10.1016/j.ccell.2017.06.004

6 Christian S., et al. (2019) **The novel dihydroorotate dehydrogenase (DHODH) inhibitor BAY 2402234 triggers differentiation and is effective in the treatment of myeloid malignancies** *Leukemia* **33**:2403–2415 https://doi.org/10.1038/s41375-019-0461-5

7 Sykes D. B., et al. (2016) **Inhibition of Dihydroorotate Dehydrogenase Overcomes Differentiation Blockade in Acute Myeloid Leukemia** *Cell* **167**:171–186 https://doi.org/10.1016/j.cell.2016.08.057

8 Wang X., et al. (2019) **Targeting pyrimidine synthesis accentuates molecular therapy response in glioblastoma stem cells** *Science Translational Medicine* **11** https://doi.org/10.1126/scitranslmed.aau4972

9 Koundinya M., et al. (2018) **Dependence on the Pyrimidine Biosynthetic Enzyme DHODH Is a Synthetic Lethal Vulnerability in Mutant KRAS-Driven Cancers** *Cell Chemical Biology* **25**:705–717 https://doi.org/10.1016/j.chembiol.2018.03.005

10 Santana-Codina N., et al. (2018) **Oncogenic KRAS supports pancreatic cancer through regulation of nucleotide synthesis** *Nat Commun* **9** https://doi.org/10.1038/s41467-018-07472-8

11 Brown K. K., Spinelli J. B., Asara J. M., Toker A. (2017) **Adaptive Reprogramming of De Novo Pyrimidine Synthesis Is a Metabolic Vulnerability in Triple-Negative Breast Cancer** *Cancer Discovery* **7**:391–399 https://doi.org/10.1158/2159-8290.Cd-16-0611

12 Mathur D., et al. (2017) **PTEN Regulates Glutamine Flux to Pyrimidine Synthesis and Sensitivity to Dihydroorotate Dehydrogenase Inhibition** *Cancer Discovery* **7**:380–390 https://doi.org/10.1158/2159-8290.Cd-16-0612

13 Li L., et al. (2019) **Identification of DHODH as a therapeutic target in small cell lung cancer** *Science Translational Medicine* **11** https://doi.org/10.1126/scitranslmed.aaw7852

14 Bajzikova M., et al. (2019) **Reactivation of Dihydroorotate Dehydrogenase-Driven Pyrimidine Biosynthesis Restores Tumor Growth of Respiration-Deficient Cancer Cells** *Cell Metab* **29**:399–416 https://doi.org/10.1016/j.cmet.2018.10.014

15 Falzone L., Salomone S., Libra M. (2018) **Evolution of Cancer Pharmacological Treatments at the Turn of the Third Millennium** *Frontiers in Pharmacology* **9** https://doi.org/10.3389/fphar.2018.01300

16 Vaddepally R. K., Kharel P., Pandey R., Garje R., Chandra A. B. (2020) **Review of Indications of FDA-Approved Immune Checkpoint Inhibitors per NCCN Guidelines with the Level of Evidence** *Cancers (Basel)* **12** https://doi.org/10.3390/cancers12030738

17 Mundry C. S., Eberle K. C., Singh P. K., Hollingsworth M. A., Mehla K. (2020) **Local and systemic immunosuppression in pancreatic cancer: Targeting the stalwarts in tumor's arsenal** *Biochim Biophys Acta Rev Cancer* **1874** https://doi.org/10.1016/j.bbcan.2020.188387

18 Waldman A. D., Fritz J. M., Lenardo M. J. (2020) **A guide to cancer immunotherapy: from T cell basic science to clinical practice** *Nat Rev Immunol* **20**:651–668 https://doi.org/10.1038/s41577-020-0306-5

19 Pishesha N., Harmand T. J., Ploegh H. L. (2022) **A guide to antigen processing and presentation** *Nature Reviews Immunology* **22**:751–764 https://doi.org/10.1038/s41577-022-00707-2

20 Cornel A. M., Mimpen I. L., Nierkens S. (2020) **MHC Class I Downregulation in Cancer: Underlying Mechanisms and Potential Targets for Cancer Immunotherapy** *Cancers (Basel)* **12** https://doi.org/10.3390/cancers12071760

21 Dhatchinamoorthy K., Colbert J. D., Rock K. L. (2021) **Cancer Immune Evasion Through Loss of MHC Class I Antigen Presentation** *Front Immunol* **12** https://doi.org/10.3389/fimmu.2021.636568

22 Han P., et al. (2019) **Genome-Wide CRISPR Screening Identifies JAK1 Deficiency as a Mechanism of T-Cell Resistance** *Front Immunol* **10** https://doi.org/10.3389/fimmu.2019.00251

23 Zaretsky J. M., et al. (2016) **Mutations Associated with Acquired Resistance to PD-1 Blockade in Melanoma** *N Engl J Med* **375**:819–829 https://doi.org/10.1056/NEJMoa1604958

24 Yamamoto K., et al. (2020) **Autophagy promotes immune evasion of pancreatic cancer by degrading MHC-I** *Nature* **581**:100–105 https://doi.org/10.1038/s41586-020-2229-5

25 Goel S., et al. (2017) **CDK4/6 inhibition triggers anti-tumour immunity** *Nature* **548**:471–475 https://doi.org/10.1038/nature23465

26 Kalbasi A., et al. (2020) **Uncoupling interferon signaling and antigen presentation to overcome immunotherapy resistance due to JAK1 loss in melanoma** *Sci Transl Med* **12** https://doi.org/10.1126/scitranslmed.abb0152

27 Gu S. S., et al. (2021) **Therapeutically Increasing MHC-I Expression Potentiates Immune Checkpoint Blockade** *Cancer Discov* **11**:1524–1541 https://doi.org/10.1158/2159-8290.Cd-20-0812

28 Rodig S. J., et al. (2018) **MHC proteins confer differential sensitivity to CTLA-4 and PD-1 blockade in untreated metastatic melanoma** *Sci Transl Med* **10** https://doi.org/10.1126/scitranslmed.aar3342

29 Liu D., et al. (2019) **Integrative molecular and clinical modeling of clinical outcomes to PD1 blockade in patients with metastatic melanoma** *Nature Medicine* **25**:1916–1927 https://doi.org/10.1038/s41591-019-0654-5

30 Grasso C. S., et al. (2020) **Conserved Interferon-γ Signaling Drives Clinical Response to Immune Checkpoint Blockade Therapy in Melanoma** *Cancer Cell* **38**:500–515 https://doi.org/10.1016/j.ccell.2020.08.005

31 Shklovskaya E., et al. (2020) **Tumor MHC Expression Guides First-Line Immunotherapy Selection in Melanoma** *Cancers (Basel)* **12** https://doi.org/10.3390/cancers12113374

32 Luthra P., et al. (2018) **Inhibiting pyrimidine biosynthesis impairs Ebola virus replication through depletion of nucleoside pools and activation of innate immune responses** *Antiviral Res* **158**:288–302 https://doi.org/10.1016/j.antiviral.2018.08.012

33 Lucas-Hourani M., et al. (2013) **Inhibition of Pyrimidine Biosynthesis Pathway Suppresses Viral Growth through Innate Immunity** *PLOS Pathogens* **9** https://doi.org/10.1371/journal.ppat.1003678

34 Sprenger H.-G., et al. (2021) **Cellular pyrimidine imbalance triggers mitochondrial DNA–dependent innate immunity** *Nature Metabolism* **3**:636–650 https://doi.org/10.1038/s42255-021-00385-9

35 Liberzon A., et al. (2011) **Molecular signatures database (MSigDB) 3.0** *Bioinformatics* **27**:1739–1740 https://doi.org/10.1093/bioinformatics/btr260

36 Subramanian A., et al. (2005) **Gene set enrichment analysis: A knowledge-based approach for interpreting genome-wide expression profiles** *Proceedings of the National Academy of Sciences* **102**:15545–15550 https://doi.org/10.1073/pnas.0506580102

37 Mullen N. J., et al. (2023) **ENT1 blockade by CNX-774 overcomes resistance to DHODH inhibition in pancreatic cancer** *Cancer Letters* **552** https://doi.org/10.1016/j.canlet.2022.215981

38 Tan Justin L., et al. (2016) **Stress from Nucleotide Depletion Activates the Transcriptional Regulator HEXIM1 to Suppress Melanoma** *Molecular Cell* **62**:34–46 https://doi.org/10.1016/j.molcel.2016.03.013

39 Zhou F. (2009) **Molecular Mechanisms of IFN-γ to Up-Regulate MHC Class I Antigen Processing and Presentation** *International Reviews of Immunology* **28**:239–260 https://doi.org/10.1080/08830180902978120

40 Dejardin E., et al. (1998) **Regulation of major histocompatibility complex class I expression by NF-κB-related proteins in breast cancer cells** *Oncogene* **16**:3299–3307 https://doi.org/10.1038/sj.onc.1201879

41 Li A., et al. (2019) **Activating cGAS-STING pathway for the optimal effect of cancer immunotherapy** *Journal of Hematology & Oncology* **12** https://doi.org/10.1186/s13045-019-0721-x

42 Thomson D. W., et al. (2019) **Discovery of GSK8612, a Highly Selective and Potent TBK1 Inhibitor** *ACS Medicinal Chemistry Letters* **10**:780–785 https://doi.org/10.1021/acsmedchemlett.9b00027

43 Podolin P. L., et al. (2005) **Attenuation of murine collagen-induced arthritis by a novel, potent, selective small molecule inhibitor of IkappaB Kinase 2, TPCA-1 (2-[(aminocarbonyl)amino]-5-(4-fluorophenyl)-3-thiophenecarboxamide), occurs via reduction of proinflammatory cytokines and antigen-induced T cell Proliferation** *J Pharmacol Exp Ther* **312**:373–381 https://doi.org/10.1124/jpet.104.074484

44 Burke J. R., et al. (2003) **BMS-345541 is a highly selective inhibitor of I kappa B kinase that binds at an allosteric site of the enzyme and blocks NF-kappa B-dependent transcription in mice** *J Biol Chem* **278**:1450–1456 https://doi.org/10.1074/jbc.M209677200

45 Napoleon J. V., et al. (2022) **Small-molecule IKKβ activation modulator (IKAM) targets MAP3K1 and inhibits pancreatic tumor growth** *Proceedings of the National Academy of Sciences* **119** https://doi.org/10.1073/pnas.2115071119

46 Yeo H., Lee Y. H., Koh D., Lim Y., Shin S. Y. (2020) **Chrysin Inhibits NF-κB-Dependent CCL5 Transcription by Targeting IκB Kinase in the Atopic Dermatitis-Like Inflammatory Microenvironment** *Int J Mol Sci* **21** https://doi.org/10.3390/ijms21197348

47 Davis M. I., et al. (2011) **Comprehensive analysis of kinase inhibitor selectivity** *Nat Biotechnol* **29**:1046–1051 https://doi.org/10.1038/nbt.1990

48 Price D. H. (2000) **P-TEFb, a cyclin-dependent kinase controlling elongation by RNA polymerase II** *Mol Cell Biol* **20**:2629–2634 https://doi.org/10.1128/mcb.20.8.2629-2634.2000

49 Ni Z., et al. (2008) **P-TEFb is critical for the maturation of RNA polymerase II into productive elongation in vivo** *Mol Cell Biol* **28**:1161–1170 https://doi.org/10.1128/mcb.01859-07

50 Chao S.-H., et al. (2000) **Flavopiridol inhibits P-TEFb and blocks HIV-1 replication** *Journal of Biological Chemistry* **275**:28345–28348

51 McPartland R. P., Wang M. C., Bloch A., Weinfeld H. (1974) **Cytidine 5'-triphosphate synthetase as a target for inhibition by the antitumor agent 3-deazauridine** *Cancer Res* **34**:3107–3111

52 Nilson Kyle A., et al. (2015) **THZ1 Reveals Roles for Cdk7 in Co-transcriptional Capping and Pausing** *Molecular Cell* **59**:576–587 https://doi.org/10.1016/j.molcel.2015.06.032

53 King H. M., et al. (2021) **Aminopyrazole based CDK9 PROTAC sensitizes pancreatic cancer cells to venetoclax** *Bioorg Med Chem Lett* **43** https://doi.org/10.1016/j.bmcl.2021.128061

54 Twyman-Saint Victor C., et al. (2015) **Radiation and dual checkpoint blockade activate non-redundant immune mechanisms in cancer** *Nature* **520**:373–377 https://doi.org/10.1038/nature14292

55 Dexter D. L., et al. (1985) **Activity of a novel 4-quinolinecarboxylic acid, NSC 368390 [6-fluoro-2-(2'-fluoro-1,1'-biphenyl-4-yl)-3-methyl-4-quinolinecarb oxylic acid sodium salt], against experimental tumors** *Cancer Res* **45**:5563–5568

56 Klotz L., et al. (2019) **Teriflunomide treatment for multiple sclerosis modulates T cell mitochondrial respiration with affinity-dependent effects** *Science Translational Medicine* **11** https://doi.org/10.1126/scitranslmed.aao5563

57 Fox R. I., et al. (1999) **Mechanism of action for leflunomide in rheumatoid arthritis** *Clin Immunol* **93**:198–208 https://doi.org/10.1006/clim.1999.4777

58 Miller A. E. (2021) **An updated review of teriflunomide's use in multiple sclerosis** *Neurodegener Dis Manag* **11**:387–409 https://doi.org/10.2217/nmt-2021-0014

59 Shin D. S., et al. (2017) **Primary Resistance to PD-1 Blockade Mediated by JAK1/2 Mutations** *Cancer Discov* **7**:188–201 https://doi.org/10.1158/2159-8290.Cd-16-1223

60 Dersh D., et al. (2021) **Genome-wide Screens Identify Lineage- and Tumor-Specific Genes Modulating MHC-I- and MHC-II-Restricted Immunosurveillance of Human Lymphomas** *Immunity* **54**:116–131 https://doi.org/10.1016/j.immuni.2020.11.002

61 Petroni G., Buqué A., Zitvogel L., Kroemer G., Galluzzi L. (2021) **Immunomodulation by targeted anticancer agents** *Cancer Cell* **39**:310–345 https://doi.org/10.1016/j.ccell.2020.11.009

62 Keshet R., et al. (2020) **Targeting purine synthesis in ASS1-expressing tumors enhances the response to immune checkpoint inhibitors** *Nature Cancer* **1**:894–908 https://doi.org/10.1038/s43018-020-0106-7

63 Olou A. A., King R. J., Yu F., Singh P. K. (2020) **MUC1 oncoprotein mitigates ER stress via CDA-mediated reprogramming of pyrimidine metabolism** *Oncogene* **39**:3381–3395 https://doi.org/10.1038/s41388-020-1225-4

64 Dasgupta A., et al. (2020) **SIRT1-NOX4 signaling axis regulates cancer cachexia** *J Exp Med* **217** https://doi.org/10.1084/jem.20190745

65 Shukla S. K., et al. (2015) **Silibinin-mediated metabolic reprogramming attenuates pancreatic cancerinduced cachexia and tumor growth** *Oncotarget* **6**:41146–41161 https://doi.org/10.18632/oncotarget.5843

## Article and author information

**Nicholas J. Mullen**
Eppley Institute for Research in Cancer and Allied Diseases, University of Nebraska Medical Center, Omaha, NE 68198-5950, USA
ORCID iD: 0000-0002-5045-0814

**Surendra K. Shukla**
Department of Oncology Science, University of Oklahoma Health Sciences Center, Oklahoma City, OK, 73014, USA

**Ravi Thakur**
Department of Oncology Science, University of Oklahoma Health Sciences Center, Oklahoma City, OK, 73014, USA

**Sai Sundeep Kollala**
Eppley Institute for Research in Cancer and Allied Diseases, University of Nebraska Medical Center, Omaha, NE 68198-5950, USA

**Dezhen Wang**
Eppley Institute for Research in Cancer and Allied Diseases, University of Nebraska Medical Center, Omaha, NE 68198-5950, USA

**Nina Chaika**
Eppley Institute for Research in Cancer and Allied Diseases, University of Nebraska Medical Center, Omaha, NE 68198-5950, USA

**Juan F. Santana**
Department of Biochemistry and Molecular Biology, University of Iowa, Iowa City, Iowa, USA

**William R. Miklavcic**
Eppley Institute for Research in Cancer and Allied Diseases, University of Nebraska Medical Center, Omaha, NE 68198-5950, USA

**Drew A. LaBreck**
Department of Oncology Science, University of Oklahoma Health Sciences Center, Oklahoma City, OK, 73014, USA

**Jayapal Reddy Mallareddy**
Eppley Institute for Research in Cancer and Allied Diseases, University of Nebraska Medical Center, Omaha, NE 68198-5950, USA

**David H. Price**
Department of Biochemistry and Molecular Biology, University of Iowa, Iowa City, Iowa, USA

**Amarnath Natarajan**
Eppley Institute for Research in Cancer and Allied Diseases, University of Nebraska Medical Center, Omaha, NE 68198-5950, USA

**Kamiya Mehla**
Department of Oncology Science, University of Oklahoma Health Sciences Center, Oklahoma City, OK, 73014, USA

**David B. Sykes**
Center for Regenerative Medicine, Massachusetts General Hospital, Boston, MA, USA, Harvard Stem Cell Institute, Cambridge, MA, USA

**Michael A. Hollingsworth**
Eppley Institute for Research in Cancer and Allied Diseases, University of Nebraska Medical Center, Omaha, NE 68198-5950, USA

**Pankaj K. Singh**
Eppley Institute for Research in Cancer and Allied Diseases, University of Nebraska Medical Center, Omaha, NE 68198-5950, USA, Department of Oncology Science, University of Oklahoma Health Sciences Center, Oklahoma City, OK, 73014, USA, Department of Pathology, University of Oklahoma Health Sciences Center, Oklahoma City, OK, 73104, USA, OU Health Stephenson Cancer Center, University of Oklahoma Health Sciences Center, Oklahoma City, OK, 73104, USA
**For correspondence:** pankaj-singh@ouhsc.edu
ORCID iD: 0000-0001-8903-0131

## Copyright



## Editors

Reviewing Editor
**Lynne-Marie Postovit**
Queens University, Kingston, Canada

Senior Editor
**Lynne-Marie Postovit**
Queens University, Kingston, Canada

**Reviewer #1 (Public Review):**

The manuscript by Mullen et al. investigated the gene expression changes in cancer cells treated with the DHODH inhibitor brequinar (BQ), to explore the therapeutic vulnerabilities induced by DHODH inhibition. The study found that BQ treatment causes upregulation of antigen presentation pathway (APP) genes and cell surface MHC class I expression, mechanistically which is mediated by the CDK9/PTEFb pathway triggered by pyrimidine nucleotide depletion. The combination of BQ and immune checkpoint therapy demonstrated a synergistic (or additive) anti-cancer effect against xenografted melanoma, suggesting the potential use of BQ and immune checkpoint blockade as a combination therapy in clinical therapeutics.

The interesting findings in the present study include demonstrating a novel cellular response in cancer cells induced by DHODH inhibition. However, whether the increased antigen presentation by DHODH inhibition actually contributed to the potentiation of the efficacy of immune-check blockade (ICB) is not directly examined is the limitation of the study. Moreover, the mechanism of the increased antigen presentation pathway by pyrimidine depletion mediated by CDK9/PTEFb was not validated by genetic KD or KO targeting by CDK9/PTEFb pathways. Finally, high concentrations of BQ have been reported to show off-target effects, sensitizing cancer cells to ferroptosis, and the authors should discuss whether the dose used in the in vivo study reached the ferroptotic sensitizing dose or not.

Comment on the revised version:

In their response letter, the authors appropriately addressed the reviewer's comments.

However, it is unfortunate that these comments are not reflected in the main text. Consequently, readers may encounter the same questions. Therefore, the reviewer recommends mentioning them in the discussion or limitations of the study, even if briefly, to address readers' concerns. Especially, addressing the comments such as the dosage of BQ being lower than the reported pro-ferroptotic dose (PMID 37407687), and the lack of examining potential impact of immune cell depletion on the efficacy of BQ treatment would be necessary for considering the proposed mechanism. The latter limitation is also raised by the other reviewer.

https://doi.org/10.7554/eLife.87292.2.sa2

**Reviewer #2 (Public Review):**

In their manuscript entitled "DHODH inhibition enhances the efficacy of immune checkpoint blockade by increasing cancer cell antigen presentation", Mullen et al. describe an interesting mechanism of inducing antigen presentation. The manuscript includes a series of experiments that demonstrate that blockade of pyrimidine synthesis with DHODH inhibitors (i.e. brequinar (BQ)) stimulates the expression of genes involved in antigen presentation. The authors provide evidence that BQ mediated induction of MHC is independent of interferon signaling. A subsequent targeted chemical screen yielded evidence that CDK9 is the critical downstream mediator that induces RNA Pol II pause release on antigen presentation genes to increase expression. Finally, the authors demonstrate that BQ elicits strong anti-tumor activity in vivo in syngeneic models, and that combination of BQ with immune checkpoint blockade (ICB) results in significant lifespan extension in the B16-F10 melanoma model. Overall, the manuscript uncovers an interesting and unexpected mechanism that influences antigen presentation and provides an avenue for pharmacological manipulation of MHC genes, which is therapeutically relevant in many cancers. However, a few key experiments are needed to ensure that the proposed mechanism is indeed functional in vivo.

Major Points:

(1) According to the proposed model, BQ mediated induction of antigen presentation is a contributing factor to the efficacy of this therapeutic strategy. If this is true, then depletion of immune cells should reduce the therapeutic efficacy of BQ in vivo. The authors should perform the B16-F10 transplant experiments in either Rag null mice (if available) or with CD8/CD4 depletion. The expectation would be that T cell depletion (or MHC loss with genetic manipulation) should reduce the efficacy of BQ treatment. Absent this critical experiment, it is difficult to confidently conclude that induction of antigen presentation is a fundamental component of the in vivo response to DHODH inhibition.

(2) Does BQ treatment induce antigen presentation in non-malignant cells? APCs? If the induction of antigen presentation is not cancer specific and related to a pyrimidine depletion stress response, then there is a possibility that healthy tissues will also exhibit a similar phenotype, raising concerns about the specificity of a de novo immune response. The authors should examine antigen presentation genes in healthy tissues treated with BQ.

(3) In the title, the authors claim that DHODH enhances the efficacy of ICB. However, the experiment shown in Figure 5D does not demonstrate this. The Kaplan Meier curves reflect more of an additive response versus a synergistic combination. Furthermore, the concurrent treatment of BQ and ICB seems to inhibit the efficacy of ICB due to BQ toxicity in immune cells. When concurrently administered, the survival of the mice is the same as with brequinar alone, suggesting that the efficacy of ICB was diminished. However, if ICB is administered following an initial dose of BQ, there is an added survival benefit of a

magnitude that is similar to ICB alone. This result seems to contradict the title. Furthermore, the authors should show the longitudinal growth curves of these tumors.

(4) Related to Point 3, the temporal separation of BQ and ICB raises the question of whether the induction of antigen presentation with BQ is persistent during the course of delayed ICB treatment. One explanation for the results is that BQ treatment reduces tumor burden, and then a subsequent course of ICB also reduces tumor burden but not that the two therapies are functioning in synergy. To address this, the authors should measure the duration of BQ mediated induction of antigen presentation after stopping treatment.

(5) In Figure 1, the authors show that DHODH inhibition induces expression of both MHC-I and MHC-II genes at the RNA level. However, they only validate MHC-I by flow cytometry. A simple experiment to evaluate the effect of BQ treatment on MHC-II surface expression would provide important additional mechanistic insight into the immunomodulatory effects of DHODH inhibition, especially given recent literature reinforcing the importance of MHC-II expression on epithelial cancers, including melanoma (Oliveira et al. Nature 2022).

Minor Points:

(1) The authors show ChIP-seq tracks from Tan et al. for HLA-B. However, given the pervasive effect of Ter treatment across many HLA genes, the authors should either show tracks at additional loci, or provide a heatmap of read density across more loci. This would substantiate the mechanistic claim that RNA Pol II occupancy and activity across antigen presentation genes is the major driver of response to DHODH inhibition as opposed to mRNA stabilization/increased translation.

(2) A compelling way to demonstrate a change in antigen presentation is through mass spectrometry based immunopeptidomics. Performing immunopeptidomic analysis of BQ treated cell lines would provide substantial mechanistic insight into the outcome of BQ treatment. While this approach may be outside the scope of the current work, the authors should speculate on how this treatment may specifically alter the antigenic landscape where future directions would include empirical immunopeptidomics measurements.

(3) While the signaling through CDK9 seems convincing, it still does not provide a mechanistic link between depleted pyrimidines and CDK9 activity. The authors should speculate on the mechanism that signals to CDK9.

(4) Related to minor point 2, the authors should consider a genetic approach to confirm the importance of CDK9. While the pharmacological approach, including multiple mechanistically distinct CDK9 inhibitors provides strong evidence, an additional experiment with genetic depletion of CDK9 (CRISPR KO, shRNA, etc) would provide compelling mechanistic confirmation.

(5) The authors should comment in the discussion on how this strategy may be particularly useful in patients harboring genetic or epigenetic loss of interferon signaling, a known mechanism of ICB resistance. Perhaps DHODH inhibition could rescue MHC expression in cells that are deficient in interferon sensing.

Overall, the paper is clearly written and presented. With the additional experiments described above, especially in vivo, this manuscript would provide a strong contribution to the field of antigen presentation in cancer. The distinct mechanisms by which DHODH inhibition induces antigen presentation will also set the stage for future exploration into alternative methods of antigen induction.

Comments on latest version:

The authors address the majority of the points raised in my previous review. However, no additional in vivo experiments were performed, which seems necessary for the major conclusions of the paper.

I disagree with the authors' assessment of Major Point 3 in my review. I have updated the text of Major Point 3 in my public review to further clarify my position.

My final assessment is that if the authors want to claim that DHODH inhibition potentiates immune checkpoint blockade, as is stated in the title, then further in vivo experimentation is needed.

https://doi.org/10.7554/eLife.87292.2.sa1

**Reviewer #3 (Public Review):**

Mullen et al present an important study describing how DHODH inhibition enhances efficacy of immune checkpoint blockade by increasing cell surface expression of MHC I in cancer cells. DHODH inhibitors have been used in the clinic for many years to treat patients with rheumatoid arthritis and there has been a growing interest in repurposing these inhibitors as anti-cancer drugs. In this manuscript, the Singh group builds on their previous work defining combinatorial strategies with DHODH inhibitors to improve efficacy. The authors identify an increased expression of genes in the antigen presentation pathway and MHC I after BQ treatment which is mediated strictly by pyrimidine depletion and CDK9/P-TEFb. The authors rationalize that increased MHC I expression induced by DHODH inhibition might favor efficacy of dual immune checkpoint blockade. In fact, this combinatorial treatment prolonged survival in an immunocompetent B16F10 melanoma model.

Previous studies have shown that DHODH inhibitors can increase expression of innate immunity-related genes but the role of DHODH and pyrimidine nucleotides in antigen presentation has not been previously reported. A strength of the manuscript is the solid in vitro mechanistic data supported by analysis in multiple cell lines. The in vivo data show compelling additive effects of DHODH inhibitors and ICB. However, more controls and experiments would be required to define the nature of these effects and to confirm that the mechanistic in vitro data is conserved in vivo.

This is a relevant manuscript proposing a mechanistic link between pyrimidine depletion and MHC I expression and a novel therapeutic approach combining DHODH inhibitors with dual checkpoint blockade. These results might be relevant for the clinical development of DHODH inhibitors in the treatment of solid tumors, a setting where these have not shown optimal efficacy yet.

Comments on revised version:

The authors have addressed my questions regarding validation of gene expression in other cell lines. They have also provided an explanation about why in vivo evaluations could not be performed for the experiment in Figure 5E.

https://doi.org/10.7554/eLife.87292.2.sa0

**Author Response**

The following is the authors’ response to the previous reviews.

> ***eLife assessment***
>
> *This important study reports a novel mechanism linking DHODH inhibition-mediated pyrimidine nucleotide depletion to antigen presentation. Alternative means of inducing antigen presentation provide therapeutic opportunities to augment immune checkpoint blockade for cancer treatment. While the solid mechanistic data in vitro are compelling, in vivo assessments of the functional relevance of this mechanism are still incomplete.*

We thank all Reviewers for their insightful comments and excellent suggestions.

> ***Reviewer #1 (Public Review):***
>
> *The manuscript by Mullen et al. investigated the gene expression changes in cancer cells treated with the DHODH inhibitor brequinar (BQ), to explore the therapeutic vulnerabilities induced by DHODH inhibition. The study found that BQ treatment causes upregulation of antigen presentation pathway (APP) genes and cell surface MHC class I expression, mechanistically which is mediated by the CDK9/PTEFb pathway triggered by pyrimidine nucleotide depletion.*

No comment from authors

> *The combination of BQ and immune checkpoint therapy demonstrated a synergistic (or additive) anti-cancer effect against xenografted melanoma, suggesting the potential use of BQ and immune checkpoint blockade as a combination therapy in clinical therapeutics.*

No comment from authors

> *The interesting findings in the present study include demonstrating a novel cellular response in cancer cells induced by DHODH inhibition. However, whether the increased antigen presentation by DHODH inhibition actually contributed to the potentiation of the efficacy of immune-check blockade (ICB) is not directly examined is the limitation of the study.*

No comment from authors for preceding text, comment addresses the following text

> *Moreover, the mechanism of the increased antigen presentation pathway by pyrimidine depletion mediated by CDK9/PTEFb was not validated by genetic KD or KO targeting by CDK9/PTEFb pathways.*

We appreciate this comment, and we would like to explain why we did not pursue these approaches. According to DepMap, CRISPR/Cas9-mediated knockout of CDK9 in cancer cell lines is almost universally deleterious, scoring as “essential” in 99.8% (1093/1095) of all cell lines tested (see Author response image 1 below). This makes sense, as P-TEFb is required for productive RNA polymerase II elongation of most mammalian genes. As such, it was not feasible to generate cell lines with stable genetic knockout of CDK9 to test our hypothesis.

While knockdown of CDK9 by RNA interference could support our results, DepMap data seems to indicate that RNAi-mediated knockdown of CDK9 is generally ineffective in silencing its activity, as this perturbation scored as “essential” in only 6.2% (44/710) of tested cell lines. This suggests that incomplete depletion of CDK9 will likely not be sufficient to block APP induction downstream of nucleotide depletion. Furthermore, RNAi-mediated depletion of CDK9 may trigger transcriptional changes in the cell by virtue of its many documented

> ***Public Reviews:***

We thank all Reviewers for their insightful comments and excellent suggestions.

> ***Reviewer #1 (Public Review):***
>
> *The manuscript by Mullen et al. investigated the gene expression changes in cancer cells treated with the DHODH inhibitor brequinar (BQ), to explore the therapeutic vulnerabilities induced by DHODH inhibition. The study found that BQ treatment causes upregulation of antigen presentation pathway (APP) genes and cell surface MHC class I expression, mechanistically which is mediated by the CDK9/PTEFb pathway triggered by pyrimidine nucleotide depletion.*

No comment from authors

> *The combination of BQ and immune checkpoint therapy demonstrated a synergistic (or additive) anti-cancer effect against xenografted melanoma, suggesting the potential use of BQ and immune checkpoint blockade as a combination therapy in clinical therapeutics.*

No comment from authors

> *The interesting findings in the present study include demonstrating a novel cellular response in cancer cells induced by DHODH inhibition. However, whether the increased antigen presentation by DHODH inhibition actually contributed to the potentiation of the efficacy of immune-check blockade (ICB) is not directly examined is the limitation of the study.*

No comment from authors for preceding text, comment addresses the following text

> *Moreover, the mechanism of the increased antigen presentation pathway by pyrimidine depletion mediated by CDK9/PTEFb was not validated by genetic KD or KO targeting by CDK9/PTEFb pathways.*

We appreciate this comment, and we would like to explain why we did not pursue these approaches. According to DepMap, CRISPR/Cas9-mediated knockout of CDK9 in cancer cell lines is almost universally deleterious, scoring as “essential” in 99.8% (1093/1095) of all cell lines tested (see Author response image 1 below). This makes sense, as P-TEFb is required for productive RNA polymerase II elongation of most mammalian genes. As such, it was not feasible to generate cell lines with stable genetic knockout of CDK9 to test our hypothesis.

While knockdown of CDK9 by RNA interference could support our results, DepMap data seems to indicate that RNAi-mediated knockdown of CDK9 is generally ineffective in silencing its activity, as this perturbation scored as “essential” in only 6.2% (44/710) of tested cell lines. This suggests that incomplete depletion of CDK9 will likely not be sufficient to block APP induction downstream of nucleotide depletion. Furthermore, RNAi-mediated depletion of CDK9 may trigger transcriptional changes in the cell by virtue of its many documented protein-protein interactions, and it would be difficult to establish a consistent “time zero” at which point CDK9 protein depletion is substantial but secondary effects of this have not yet occurred to a significant degree. These factors constitute major limitations of experiments using RNAi-mediated knockdown of CDK9.

**Author response image 1.**

Essentiality score from CRISPR and RNAi perturbation of CDK9 in cancer cell lines https://depmap.org/portal/gene/CDK9?tab=overview&dependency=RNAi_merged

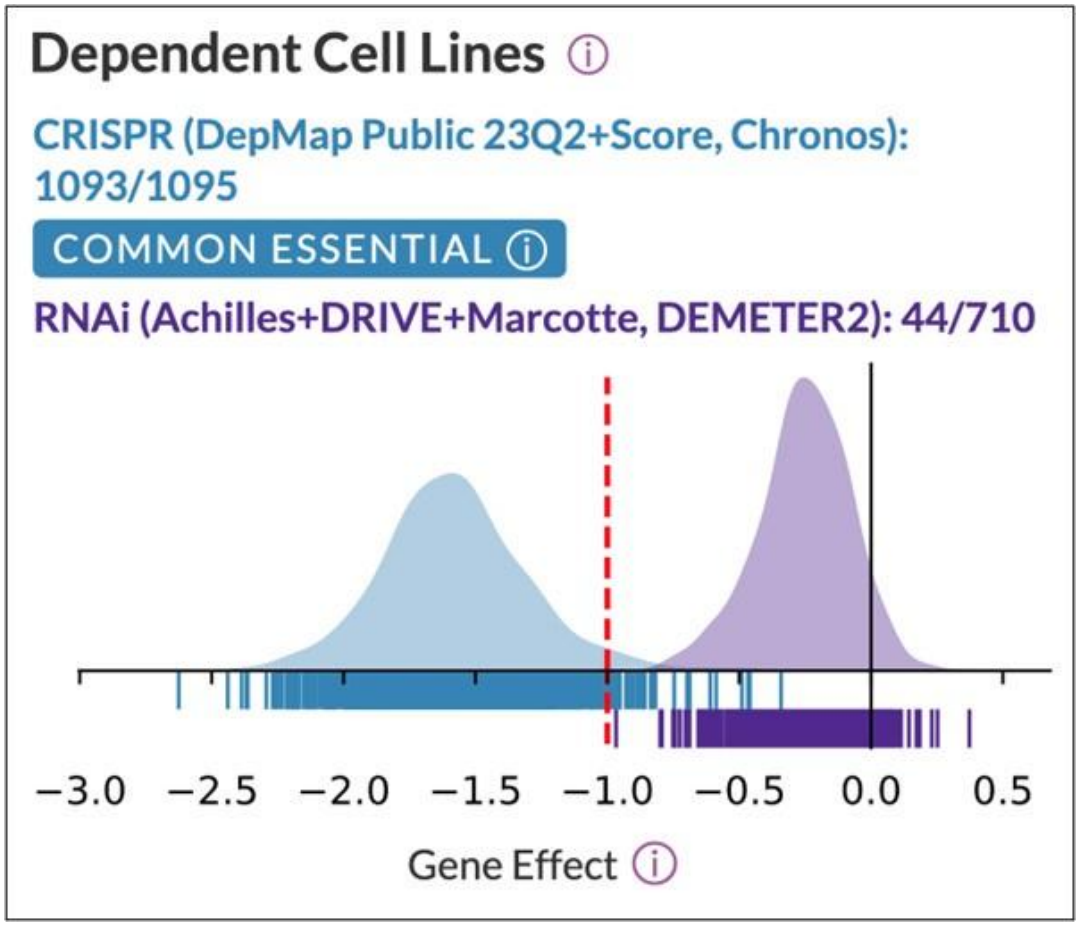


At any rate, we provide evidence that three different inhibitors of CDK9 (flavopiridol, dinaciclib, and AT7519) all inhibit our effect of interest (Fig 4B). The same results were observed using a previously validated CDK9-directed proteolysis targeting chimera (PROTAC2), and this was reversed by addition of excess pomalidomide (Fig 4C), which correlated with the presence/absence of CDK9 on western blot under the exact same conditions (Fig 4D).

It is formally possible that all CDK9 inhibitors we tested are blocking BQ-mediated APP induction by some shared off-target mechanism (or perhaps by two or more different off-target mechanisms) AND this CDK9-independent target also happens to be degraded by PROTAC2. However, this would be an extraordinarily non-parsimonious explanation for our results, and so we contend that we have provided compelling evidence for the requirement of CDK9 for BQ-mediated APP induction.

> *Finally, high concentrations of BQ have been reported to show off-target effects, sensitizing cancer cells to ferroptosis, and the authors should discuss whether the dose used in the in vivo study reached the ferroptotic sensitizing dose or not.*

We are intrigued by the results shown to us by Reviewer #1 in the linked preprint (Mishima et al 2022, https://doi.org/10.21203/rs.3.rs-2190326/v1). We have also observed in our

unpublished data that very high concentrations of BQ (>150μM) cause loss of cell viability that is not rescued by uridine supplementation and that occurs even in DHODH knockout cells. This effect of high-dose BQ must be DHODH-independent. We also agree that Mishima et al provide compelling evidence that the ferroptosis-sensitizing effect of high-dose BQ treatment is due (at least in large part) to inhibition of FSP1.

Although we showed that DHODH is strongly inhibited in tumor cells in vivo (Fig 5C), we did not directly measure the concentration of BQ in the tumor or plasma. Sykes et al (PMID: 27641501) found that the maximum plasma concentration (Cmax) for [BQ]free following a single IP administration in C57Bl6/J mice (15mg/kg) is approximately 3μM, while the Cmax for [BQ]total was around 215μM. Because polar drug molecules bound to serum proteins (predominantly albumin) are not available to bind other targets, [BQ]free is the relevant parameter.

Given a Cmax for [BQ]free of 3μM and half-life of 12.0 hours, we estimate that the steady-state [BQ]free with daily IP injections at this dose is around 4μM. Since we used an administration schedule of 10mg/kg every 24 hours, we estimate that the steady-state plasma [BQ]free in our system was 2.67μM (assuming initial Cmax of 2μM and half-life of 12.0 hours).

To derive an upper-bound estimate for the Cmax of [BQ]free over the 12-day treatment period (Fig 5A-D), we will use the observed data for 15mg/kg dose, and we will assume that 1) there is no clearance of BQ whatsoever and 2) that [BQ]free increases linearly with increasing [BQ]total. This yields a maximum free BQ concentration of 12 x 3 = 36μM.

Therefore, we consider it very unlikely that plasma concentrations of free BQ in our experiment exceeded the lower limit of the ferroptosis-sensitizing dose range reported by Mishima et al. However, without direct pharmacokinetic analysis, we cannot say for sure what the maximal [BQ]free was under our experimental conditions.

> ***Reviewer #2 (Public Review):***
>
> *In their manuscript entitled "DHODH inhibition enhances the efficacy of immune checkpoint blockade by increasing cancer cell antigen presentation", Mullen et al. describe an interesting mechanism of inducing antigen presentation. The manuscript includes a series of experiments that demonstrate that blockade of pyrimidine synthesis with DHODH inhibitors (i.e. brequinar (BQ)) stimulates the expression of genes involved in antigen presentation. The authors provide evidence that BQ mediated induction of MHC is independent of interferon signaling. A subsequent targeted chemical screen yielded evidence that CDK9 is the critical downstream mediator that induces RNA Pol II pause release on antigen presentation genes to increase expression. Finally, the authors demonstrate that BQ elicits strong anti-tumor activity in vivo in syngeneic models, and that combination of BQ with immune checkpoint blockade (ICB) results in significant lifespan extension in the B16-F10 melanoma model. Overall, the manuscript uncovers an interesting and unexpected mechanism that influences antigen presentation and provides an avenue for pharmacological manipulation of MHC genes, which is therapeutically relevant in many cancers. However, a few key experiments are needed to ensure that the proposed mechanism is indeed functional in vivo.*
>
> *The combination of DHODH inhibition with ICB reflects more of an additive response instead of a synergistic combination. Moreover, the temporal separation of BQ and ICB raises the question of whether the induction of antigen presentation with BQ is persistent during the course of delayed ICB treatment. To confidently conclude that induction of antigen presentation is a fundamental component of the in vivo response to DHODH inhibition, the authors should examine whether depletion of immune cells can reduce the therapeutic efficacy of BQ in vivo.*

We concur with this assessment.

> *Moreover, they should examine whether BQ treatment induces antigen presentation in non-malignant cells and APCs to determine the cancer specificity.*

Although we showed that this occurs in HEK-293T cells, we appreciate that this cell line is not representative of human cells of any organ system in vivo. So, we agree it is important to determine if DHODH inhibition induces antigen presentation in human tissues and professional antigen presenting cells, and this is an excellent focus for future studies.

However, it should also be noted that increased antigen presentation in non-malignant host tissues would not be expected to generate an autoimmune response, because host tissues likely lack strong neoantigens, and whatever immunogenic peptides they may have would likely be presented via MHC-I at baseline (i.e. even in the absence of DHODH inhibitor treatment), since all nucleated cells express MHC-I.

This argument is strongly supported by clinical experience/data, as DHODH inhibitors (leflunomide and teriflunomide) are commonly used to treat rheumatoid arthritis and multiple sclerosis. While the pathophysiology of these autoimmune syndromes is complex, it is thought that both diseases are driven by aberrant T-cell attack on host tissues, mediated by incorrect recognition of host antigens presented via MHC-I (as well as MHC-II) as "foreign."

If increased antigen presentation in host tissues (downstream of DHODH inhibition) could lead to a de novo autoimmune response, then administration of DHODH inhibitors would be expected to exacerbate T-cell driven autoimmune disease rather than ameliorate it. Randomized controlled trials have consistently found that treatment with DHODH inhibitors leads to improvement of rheumatoid arthritis and multiple sclerosis symptoms, which is the opposite of what one would expect if DHODH inhibitors are causing de novo autoimmune reactions in human patients.

> *Finally, although the authors show that DHODH inhibition induces expression of both MHC-I and MHC-II genes at the RNA level, only MHC-I is validated by flow cytometry given the importance of MHC-II expression on epithelial cancers, including melanoma, MHC-II should be validated as well.*

We fully agree with this statement. We attempted to quantify cell surface MHC-II expression by FACS using the same method as for MHC-I (Figs 1G-H, 2D, and 3F). We did not detect cell surface MHC-II in any of our cancer cell lines, despite the use of high-dose interferon gamma and other stimulants (which robustly increase MHC-II mRNA in our system) in an attempt to induce expression. However, because we did not use cells known to express MHC-II as a positive control (e.g. B-cell leukemia cell lines or primary splenocytes), we do not know if our results are due to some technical failure (perhaps related to our protocol/reagents) or if they reflect a true absence of cell surface MHC-II in our cell lines.

If the latter is true, that implies that either 1) MHC-II mRNA is not translated or 2) that it is translated, but our cancer cell lines lack one or more elements of the machinery required for MHC-II antigen presentation.

In any case, it is important to determine if DHODH inhibition increases MHC-II at the cell surface of cancer cells using appropriate positive and negative controls, as this could have important implications for cancer immunotherapy.

[As a minor point, melanoma is not an epithelial cancer, as it is derived from neural crest lineage cells (melanocytes)]

> *Overall, the paper is clearly written and presented. With the additional experiments described above, especially in vivo, this manuscript would provide a strong contribution to the field of antigen presentation in cancer. The distinct mechanisms by which DHODH inhibition induces antigen presentation will also set the stage for future exploration into alternative methods of antigen induction.*
>
> ***Reviewer #3 (Public Review):***
>
> *Mullen et al present an important study describing how DHODH inhibition enhances efficacy of immune checkpoint blockade by increasing cell surface expression of MHC I in cancer cells. DHODH inhibitors have been used in the clinic for many years to treat patients with rheumatoid arthritis and there has been a growing interest in repurposing these inhibitors as anti-cancer drugs. In this manuscript, the Singh group build on their previous work defining combinatorial strategies with DHODH inhibitors to improve efficacy. The authors identify an increase in expression of genes involved in the antigen presentation pathway and MHC I after BQ treatment and they narrow the mechanism to be strictly pyrimidine and CDK9/P-TEFb dependent. The authors rationalize that increased MHC I expression induced by DHODH inhibition might favor efficacy of dual immune checkpoint blockade. This combinatorial treatment prolonged survival in an immunocompetent B16F10 melanoma model.*

[No comment from authors]

> *Previous studies have shown that DHODH inhibitors can increase expression of innate immunity-related genes but the role of DHODH and pyrimidine nucleotides in antigen presentation has not been previously reported. A strength of the manuscript is the use of multiple controls across a panel of cell lines to exclude off-target effects and to confirm that effects are exclusively dependent on pyrimidine depletion. Overall, the authors do a thorough characterization of the mechanism that mediates MHC I upregulation using multiple strategies. Furthermore, the in vivo studies provide solid evidence for combining DHODH inhibitors with immune checkpoint blockade.*

No comment from authors

> *However, despite the use of multiple cell lines, most experiments are only performed in one cell line, and it is hard to understand why particular gene sets, cell lines or time points are selected for each experiment. It would be beneficial to standardize experimental conditions and confirm the most relevant findings in multiple cell lines.*

We appreciate this comment, and we understand how the use of various cell lines may seem puzzling. We would like to explain how our cell line panel evolved over the course of the study. Our first indication that BQ caused APP upregulation came from transcriptomics experiments (Figs 1A-D, S1A) performed as part of a previous study investigating BQ resistance (Mullen et al, 2023 Cancer Letters). In that study, we used CFPAC-1 as a model for BQ sensitivity and S2-013 as a model for BQ resistance. We did RNA sequencing +/- BQ in these cell lines to look for gene expression patterns that might underlie resistance/sensitivity to BQ. When analyzing this data, we serendipitously discovered the APP/MHC phenomenon, which gave rise to the present study.

Our next step was to extend these findings to cancer cell lines of other histologies, and we prioritized cell lines derived from common cancer types for which immunotherapy (specifically ICB) are clinically approved. This is why A549 (lung adenocarcinoma), HCT116 (colorectal adenocarcinoma), A375 (cutaneous melanoma), and MDA-MB-231 (triple-negative breast cancer) cell lines were introduced.

Because PDAC is considered to have an especially “immune-cold” tumor microenvironment, we reasoned that even dramatically increasing cancer cell antigen presentation may be insufficient to elicit an effective anti-tumor immune response in vivo. So we shifted our focus towards melanoma, because a subset of melanoma patients is very responsive to ICB and loss of antigen presentation (by direct silencing or homozygous loss-of-function mutations in MHC-I components such as B2M, or by functional loss of IFN-JAK1/2-STAT signaling) has been shown to mediate ICB resistance in human melanoma patients. This is why we extended our findings to B16F10 murine melanoma cells, intending to use them for in vivo studies with syngeneic immunocompetent recipient mice.

The PDAC cell line MiaPaCa2 was introduced because a collaborator at our institution (Amar Natarajan) happened to have IKK2 knockout MiaPaCa2 cells, which allowed us to genetically validate our inhibitor results showing that IKK1 and IKK2 (crucial effectors for NF-kB signaling) are dispensable for our effect of interest.

Ultimately, realizing that our results spanned various human and murine cell lines, we chose to use HEK-293T cells to validate the general applicability of our findings to proliferating cells in 2D culture, since HEK-293T cells (compared to our cancer cell lines) have relatively few genetic idiosyncrasies and express MHC-I at baseline.

> *The differential in vivo survival depending on dosing schedule is interesting. However, this section could be strengthened with a more thorough evaluation of the tumors at endpoint.*
>
> *Overall, this is an interesting manuscript proposing a mechanistic link between pyrimidine depletion and MHC I expression and a novel therapeutic strategy combining DHODH inhibitors with dual checkpoint blockade. These results might be relevant for the clinical development of DHODH inhibitors in the treatment of solid tumors, a setting where these inhibitors have not shown optimal efficacy yet.*
>
> ***Recommendations for the authors:***
>
> ***Reviewer #1 (Recommendations For The Authors):***
>
> *(1) The main issue is that it did not directly examine whether the increased antigen presentation by DHODH inhibition contributed to the potentiation of the efficacy of immune-check blockade (ICB). The additional effect of BQ in the xenograft tumor study was not examined to determine if it was due to increased antigen presentation toward the cancer cells or due to merely cell cycle arrest effect by pyrimidine depletion in the tumor cells. The different administration timing of ICB with BQ treatment (Fig 5E) would not be sufficient to answer this issue.*

We agree with this assessment and, and we believe the experiment proposed by Reviewer #2 below (comparing the efficacy of BQ in Rag-null versus immunocompetent recipients) would address this question directly. We also think that using a more immunogenic cell line for this experiment (such as B16F10 transduced with ovalbumin or some other strong neoantigen) would be useful given the poor immunogenicity and lack of any defined strong neoantigen in B16F10 cells. An orthogonal approach would be to engraft cancer cells with or without B2M knockout into immunocompetent recipient mice (+/- BQ treatment) to further implicate MHC-I and antigen presentation. These questions will be addressed in future studies.

> *(2) Additionally, in the in vivo study, the increase in surface MHC1 in the protein level in by BQ treatment was not examined in the tumor samples, and it was not confirmed whether increased antigen presentation by BQ treatment actually promoted an anti-*

> *cancer immune response in immune cells. To support the story presented in the study, these data would be necessary.*

We attempted to show this by immunohistochemistry, but unfortunately the anti-H2-Db antibody that we obtained for this purpose did not have satisfactory performance to assess this in our tissue samples harvested at necropsy.

> *(3) The mechanism of the increased antigen presentation pathway by pyrimidine depletion mediated by CDK9/PTEFb was not validated by genetic KD or KO targeting by CDK9/PTEFb pathways. In general, results only by the inhibitor assay have a limitation of off-target effects.*

Please see our above reply to Reviewer #1 comment making this same point, where we spell out our rationale for not pursuing these experiments.

> *(4) High concentrations of BQ (> 50 uM) have been reported to show off-target effects, sensitizing cancer cells to ferroptosis, an iron-mediated lipid peroxidation-dependent cell death, independent of DHODH inhibition (https://www.researchsquare.com/article/rs-2190326/v1). It would be needed to discuss whether the dose used in the in vivo study reached the ferroptotic sensitizing dose or not.*

Please see our above reply to Reviewer #1 comment making this same point, where we explain why we are very confident that the BQ dose administered in our animal experiments was far below the minimum reported BQ dose required to sensitize cancer cells to ferroptosis in vitro.

> ***Reviewer #2 (Recommendations For The Authors):***
>
> *Major Points*
>
> *(1) According to the proposed model, BQ mediated induction of antigen presentation is a contributing factor to the efficacy of this therapeutic strategy. If this is true, then depletion of immune cells should reduce the therapeutic efficacy of BQ in vivo. The authors should perform the B16-F10 transplant experiments in either Rag null mice (if available) or with CD8/CD4 depletion. The expectation would be that T cell depletion (or MHC loss with genetic manipulation) should reduce the efficacy of BQ treatment. Absent this critical experiment, it is difficult to confidently conclude that induction of antigen presentation is a fundamental component of the in vivo response to DHODH inhibition.*

We agree with this assessment and the proposed experiment comparing the response in Rag-null versus immunocompetent recipients. We also think that using a more immunogenic cell line for this experiment (such as B16F10 transduced with ovalbumin or some other strong neoantigen) would be useful given the poor immunogenicity and lack of any defined strong neoantigen in B16F10 cells. An orthogonal approach would be to engraft cancer cells with or without B2M knockout into immunocompetent recipient mice (+/- BQ treatment) to further implicate MHC-I and antigen presentation. These questions will be addressed in future studies.

> *(2) Does BQ treatment induce antigen presentation in non-malignant cells? APCs? If the induction of antigen presentation is not cancer specific and related to a pyrimidine depletion stress response, then there is a possibility that healthy tissues will also exhibit a similar phenotype, raising concerns about the specificity of a de novo immune response. The authors should examine antigen presentation genes in healthy tissues treated with BQ.*

We agree it is important to examine if our findings regarding nucleotide depletion and antigen presentation are true of APCs and other non-transformed cells, but we are not so concerned about the possibility of raising an immune response against non-malignant host tissues, as explained above. We have reproduced the relevant section below:

“However, it should also be noted that increased antigen presentation in non-malignant host tissues would not be expected to generate an autoimmune response, because host tissues likely lack strong neoantigens, and whatever immunogenic peptides they may have would likely be presented via MHC-I at baseline, since all nucleated cells express MHC-I.

This argument is strongly supported by clinical experience/data, as DHODH inhibitors (leflunomide and teriflunomide) are commonly used to treat rheumatoid arthritis and multiple sclerosis. While the pathophysiology of these autoimmune syndromes is complex, it is thought that both diseases are driven by aberrant T-cell attack on host tissues, mediated by incorrect recognition of host antigens presented via MHC-I (as well as MHC-II) as “foreign.”

If increased antigen presentation in host tissues (downstream of DHODH inhibition) could lead to a de novo autoimmune response, then administration of DHODH inhibitors would be expected to exacerbate T-cell driven autoimmune disease rather than ameliorate it. Randomized controlled trials have consistently found that treatment with DHODH inhibitors leads to improvement of rheumatoid arthritis and multiple sclerosis symptoms, which is the opposite of what one would expect if DHODH inhibitors are causing de novo autoimmune reactions in human patients.”

> *(3) In the title, the authors claim that DHODH enhances the efficacy of ICB. However, the experiment shown in Figure 5D does not demonstrate this. The Kaplan Meier curves reflect more of an additive response versus a synergistic combination. Furthermore, the concurrent treatment of BQ and ICB seems to inhibit the efficacy of ICB due to BQ toxicity in immune cells. This result seems to contradict the title.*

We do not agree with this assessment. Given that the effect of dual ICB alone was very marginal, while the effect of BQ monotherapy was quite marked, we cannot conclude from Fig 5 that BQ treatment inhibited ICB efficacy due to immune suppression.

> *(4) Related to Point 3, the temporal separation of BQ and ICB raises the question of whether the induction of antigen presentation with BQ is persistent during the course of delayed ICB treatment. One explanation for the results is that BQ treatment reduces tumor burden, and then a subsequent course of ICB also reduces tumor burden but not that the two therapies are functioning in synergy. To address this, the authors should measure the duration of BQ mediated induction of antigen presentation after stopping treatment.*

We agree that the alternative explanation proposed by Reviewer #2 is possible and we appreciate the suggestion to test the stability of APP induction after stopping BQ treatment.

> *(5) In Figure 1, the authors show that DHODH inhibition induces expression of both MHC-I and MHC-II genes at the RNA level. However, they only validate MHC-I by flow cytometry. A simple experiment to evaluate the effect of BQ treatment on MHC-II surface expression would provide important additional mechanistic insight into the immunomodulatory effects of DHODH inhibition, especially given recent literature reinforcing the importance of MHC-II expression on epithelial cancers, including melanoma (Oliveira et al. Nature 2022).*

We fully agree with this statement. We attempted to quantify cell surface MHC-II expression by FACS using the same method as for MHC-I (Figs 1G-H, 2D, and 3F). We did not detect cell surface MHC-II in any of our cancer cell lines, despite the use of high-dose interferon gamma and other stimulants (which robustly increase MHC-II mRNA in our system) in an attempt to induce expression. However, because we did not use cells known to express MHC-II as a positive control (e.g. B-cell leukemia cell lines or primary splenocytes), we do not know if our results are due to some technical failure (perhaps related to our protocol/reagents) or if they reflect a true absence of cell surface MHC-II in our cell lines.

If the latter is true, that implies that either 1) MHC-II mRNA is not translated or 2) that it is translated, but our cancer cell lines lack one or more elements of the machinery required for MHC-II antigen presentation.

In any case, it is important to determine if DHODH inhibition increases MHC-II at the cell surface of cancer cells using appropriate positive and negative controls, as this could have important implications for cancer immunotherapy.

[As a minor point, melanoma is not an epithelial cancer, as it is derived from neural crest lineage cells (melanocytes)]

> *Minor Points*
>
> *(1) The authors show ChIP-seq tracks from Tan et al. for HLA-B. However, given the pervasive effect of Ter treatment across many HLA genes, the authors should either show tracks at additional loci, or provide a heatmap of read density across more loci. This would substantiate the mechanistic claim that RNA Pol II occupancy and activity across antigen presentation genes is the major driver of response to DHODH inhibition as opposed to mRNA stabilization/increased translation.*

We appreciate this suggestion. We have changed Fig 4 by replacing the HLA-B track (old Fig 4E) with a representation of fold change (Ter/DMSO) in Pol II occupancy versus fold change (Ter/DMSO) in mRNA abundance for 23 relevant genes (new Fig 4G); both of these datasets were obtained from the Tan et al manuscript. This new figure panel (Fig 4G) also shows linear regression analysis demonstrating that Pol II occupancy and mRNA expression are significantly correlated for APP genes. While we recognize that this data in itself is not formal proof of our hypothesis, it does strongly support the notion that increased transcription is responsible for the increased mRNA abundance of APP genes that we have observed.

> *(2) A compelling way to demonstrate a change in antigen presentation is through mass spectrometry based immunopeptidomics. Performing immunopeptidomic analysis of BQ treated cell lines would provide substantial mechanistic insight into the outcome of BQ treatment. While this approach may be outside the scope of the current work, the authors should speculate on how this treatment may specifically alter the antigenic landscape where future directions would include empirical immunopeptidomics measurements.*

We fully agree with this comment. While the abundance of cancer cell surface MHC-I is an important factor for anticancer immunity, another crucial factor is the identity of peptides that are presented. Treatments that cause presentation of more immunogenic peptides can enhance T-cell recognition even in the absence of a relative change in cell surface MHC-I abundance.

While we did not perform the immunopeptidomics experiments described, we can offer some speculation regarding this comment. As shown in Fig 1D-E, transcriptomics experiments suggest that immunoproteasome subunits (PSMB8, PSMB9, PSMB10) are

upregulated upon DHODH inhibition. If this change in mRNA levels translates into greater immunoproteasome activity (which was not tested in our study), this would be expected to alter the repertoire of peptides available for presentation and could thereby change the immunopeptidome.

However, this hypothesis requires direct testing, and we hope future studies will delineate the effects of DHODH inhibition and other cancer therapies on the immunopeptidome, as this area of research will have important clinical implications.

> *(3) While the signaling through CDK9 seems convincing, it still does not provide a mechanistic link between depleted pyrimidines and CDK9 activity. The authors should speculate on the mechanism that signals to CDK9.*
>
> *We agree with the assessment. A mechanistic link between depleted pyrimidines and CDK9 activity will be a subject of future studies.*
>
> *(4) Related to minor point 2, the authors should consider a genetic approach to confirm the importance of CDK9. While the pharmacological approach, including multiple mechanistically distinct CDK9 inhibitors provides strong evidence, an additional experiment with genetic depletion of CDK9 (CRISPR KO, shRNA, etc) would provide compelling mechanistic confirmation.*

Reviewer #1 raised this very same point, and we agree. Please see our reply to Reviewer #1, which details why we did not pursue this approach and argues that the evidence we present is compelling even in absence of genetic manipulation.

Additionally, please see the new Fig 4E and 4F, which is a repeat of Fig 4B using HCT116 cells. Figure 4E shows that, in this cell line, CDK9 inhibitors (flavopiridol, dinaciclib, and AT7519) block BQ-mediated APP induction, while PROTAC2 does not. Figure 4F shows that (for reasons we cannot fully explain) PROTAC2 does not lead to CDK9 degradation in HCT116 cells. This data strongly implicates CDK9, because it excludes a CDK9-degradation-independent effect of PROTAC2.

> *(5) Figure 2B needs a legend.*

Thank you for pointing this out. We have added a legend to Fig 2B.

> *(6) The authors should comment in the discussion on how this strategy may be particularly useful in patients harboring genetic or epigenetic loss of interferon signaling, a known mechanism of ICB resistance. Perhaps DHODH inhibition could rescue MHC expression in cells that are deficient in interferon sensing.*

Thank you for this suggestion! We have amended the Discussion section to mention this important point. Please see paragraph 2 of the revised Discussion section where we have added the following text:

“Because BQ-mediated APP induction does not require interferon signaling, this strategy may have particular relevance for clinical scenarios in which tumor antigen presentation is dampened by the loss or silencing of cancer cell interferon signaling, which has been demonstrated to confer both intrinsic and acquired ICB resistance in human melanoma patients.”

> ***Reviewer #3 (Recommendations For The Authors):***
>
> *The authors present convincing evidence of the mechanism by which pyrimidine nucleotides regulate MHC I levels and about the potential of combining DHODH*

> *inhibitors with dual immune checkpoint blockade (ICB). This is an interesting paper given the clinical relevance of DHODH inhibitors. The studies raise some questions, and some points might need clarifying as below:*
>
> - *In Figure 2C, why do the authors focus on these two genes in the uridine rescue? These are important genes mediating antigen presentation, but it might be more interesting to see how H2-Db and H2-Kb expression correlate with the protein data shown in Fig 2D. Fig. 2C-2D is a relevant control, so it would be important to validate in a different cancer cell line (e.g. one of the PDAC cell lines used for the RNAseq).*

We appreciate this comment. Although Fig 3C shows that BQ-induced expression of H2-Db, H2-Kb, and B2m is reversed by uridine (in B16F10 cells), we recognize that this was not the best placement for this data, as it can easily be overlooked here since uridine reversal is not the main point of Fig 3C. We have left Fig 3C as is, because we think that the uridine reversal demonstrated in that panel serves as a good internal positive control for reversal of BQ-mediated APP induction in that experiment.

We have repeated the experiments shown in the original Fig 2C and substituted the original Fig 2C with a new Fig 2C and Fig S2B, which show both Tap1 and Nlrc5 as well as H2-Db, H2-Kb, and B2m after treatment with either BQ (new Fig 2C) or teriflunomide (new Fig S2B). The original Fig S2B is now Fig S2C, and it shows that uridine has no effect on the expression of any of the genes assayed in the new Fig 2C or S2B.

The reversibility of cell surface MHC-I induction was also validated in HCT116 cells (Fig 3F). We included the uridine reversal in Fig 3F to avoid duplicating the control and BQ FACS data in multiple panels.

We have also added the qPCR data for HCT116 cells showing this same phenotype (at the mRNA level), which is the new Fig S2D.

We decided to prioritize HCT116 cells for our mechanistic studies (Figures S2D, S4A, and 4E-F) because previous reports indicate that it is diploid and therefore less genetically deranged compared to our other cancer cell lines.

> - *Figure 2F shows an elegant experiment to discard off-target effects related to cell death and to confirm that the increased MHC I expression is uniquely dependent on pyrimidines. DHODH has recently been involved in ferroptosis, a highly immunogenic type of cell death. What are the authors' thoughts on BQ-induced ferroptosis as a possible contributor to the effects of ICB? Does BQ + ferroptosis inhibitor (ferrostatin) affect cell surface MHC I and/or expression of antigen processing genes?*

The potential role of DHODH in ferroptosis protection (Mao et al 2021) has important implications, so we are glad that multiple reviewers raised questions concerning ferroptosis. We did not directly test the effect of ferroptosis inducing agents (with or without BQ) on MHC-I/APP expression, but that is certainly a worthwhile line of investigation.

The DHODH/ferroptosis issue is complicated by a study pointed out by Reviewer #1 that challenges the role of DHODH inhibition in BQ-mediated ferroptosis sensitization (Mishima et al, 2022). This study argues that high-dose BQ treatment causes FSP1 inhibition, and this underlies the effect of BQ on the cellular response to ferroptosis-inducing agents.

Regardless of whether BQ-induced ferroptosis-sensitization is dependent on DHODH, FSP1, or some other factor, the Mao and Mishima studies agree that a relatively high dose of BQ is

required to observe these effects (100-200μM for most cell lines and >50μM even in the most ferroptosis-sensitive cell lines). As we explained above, we consider it very unlikely that the in vivo BQ exposure in our experiments (Fig 5) was high enough to cause significant ferroptosis, especially in the absence of any dedicated ferroptosis-inducing agent (which is typically required to cause ferroptosis even in the presence of high-dose BQ).

> - *The authors nail down the mechanism to CDK9 (Fig 4). However, all these experiments are performed in 293T cells. I would like to see a repeat of Fig. 4B in a cancer cell line (either PDAC or B16). Also, does BQ have any effect on CDK9 expression/protein levels?*

We have added two figure panels that address this comment (new Fig 4E and 4F). Figure 4E (which is a repeat of Fig 4B with HCT116 cells) shows that CDK9 inhibitors (flavopiridol, AT7519, and dinaciclib) reverse BQ-mediated APP induction in HCT116 cells (this agrees with Fig S4A showing that flavopiridol reverses MHC induction by various nucleotide synthesis inhibitors in this cell line), but PROTAC2 does not. Figure 4F shows that PROTAC2 (for reasons we cannot explain) does not cause CDK9 degradation in HCT116 cells. This adds further support to our thesis that CDK9 is a critical mediator of BQ-mediated APP induction (because how else can this pattern of results be explained?). The text of the Results section has been amended to reflect this.

We chose to use HCT116 cells for this repeat experiment 1) to align with Fig S4A and 2) because, as previously mentioned, we consider HCT116 to be a good cell line for mechanistic studies because of its relative lack of idiosyncratic genetic features (compared to CFPAC-1, for example, which was derived from a patient with cystic fibrosis).

> - *What are the differences in tumor size for the experiment shown in Figure 5E? What about tumor cell death in the ICB vs. BQ+ICB groups?*

Because this was a survival assay, direct comparisons of tumor volumes between groups was not possible at later time points, since mice that die or have to be euthanized are removed from their experimental group, which lowers the average group tumor burden at subsequent time points. Although tumor volume was the most common euthanasia criteria reached, a subset of mice were either found dead or had to be euthanized for other reasons attributed to their tumor burden (moribund state, inability to ambulate or stand, persistent bleeding from tumor ulceration, severe loss of body mass, etc.). This confounds any comparison of endpoint measurements (such as immunohistochemical quantification of tumor cell death markers, T-cell markers, etc.).

> - *The different response in the concurrent vs delayed treatment is very interesting. The authors suggest two possible mechanisms to explain this: "1) Concurrent BQ dampens the initial anticancer immune response generated by dual ICB, or b) cancer cell MHC-I and related genes are not maximally upregulated at the time of ICB administration with concurrent treatment". However, and despite the caveat of comparing the in vitro to the in vivo setting, Fig 2D shows upregulation of MHC I already at 24h of treatment in B16 cells. Have the authors checked T cell infiltration in the concurrent and delayed treatment setting?*

For the same reasons described in response to the preceding comment, tumors harvested upon mouse death/euthanasia from our survival experiment were not suitable for cross-cohort comparison of tumor endpoint measurements. An additional experiment in which mice are necropsied at a prespecified time point (before any mice have died or reached

euthanasia criteria, as in the experiment for Fig 5A-D) would be required to answer this question.

> - *Page 5, line 181 -do the authors mean "nucleotide salvage inhibitors" instead of "synthesis"?*

We believe the reviewer is referring to the following sentence:

“The other drugs screened included nucleotide synthesis inhibitors (5-fluorouracil, methotrexate, gemcitabine, and hydroxyurea), DNA damage inducers (oxaliplatin, irinotecan, and cytarabine), a microtubule targeting drug (paclitaxel), a DNA methylation inhibitor (azacytidine), and other small molecule inhibitors (Fig 2F).”

In this context, we believe our use of “synthesis” instead of “salvage” is correct, because methotrexate and 5-FU inhibit thymidylate synthase (which mediates de novo dTTP synthesis), while gemcitabine and hydroxyurea inhibit ribonucleotide reductase (which mediates de novo synthesis of all dNTPs).